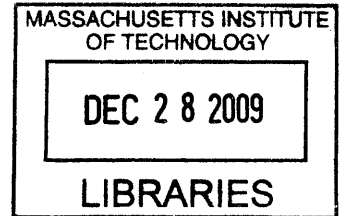


Design and Manufacturing of High Precision Roll-to-Roll Multi-layer Printing Machine- Measurement and Experiment

by

Wenzhuo Yang

B.S., Industrial Engineering and Management (2008)
Shanghai Jiaotong University



Submitted to the Department of Mechanical Engineering in partial
fulfillment of the requirements for the degree of

Master of Engineering

ARCHIVES

at the

MASSACHUSETTS INSTITUTE OF TECHNOLOGY

August 2009

© Massachusetts Institute of Technology, 2009. All rights reserved.

Signature of Author:.....

.....
Department of Mechanical Engineering
August 18, 2009

Certified by:

.....
David E. Hardt
Professor of Mechanical Engineering
Thesis Supervisor

Accepted by:.....

.....
David E. Hardt
Chairman, Departmental Committee on Graduate Studies
Department of Mechanical Engineering

Design and Manufacturing of High Precision Roll-to-Roll Multi-layer Printing - Measurement and Experiment

by

Wenzhuo Yang

Submitted to the Department of Mechanical Engineering
on 14 August, 2009, in partial fulfillment of the
requirements for the Degree of Masters of Engineering in Manufacturing

Abstract

In 2008, a prototype machine demonstrating the application of roll-to-roll technology in micro-contact printing was developed. In this research, the prototype machine was upgraded by designing and machining a device that could fabricate a flat stamp with significantly less variance. The print roll wrapping system was reconfigured in order to capture the stamp with uniform force and good alignment. The motion control for the print roller and impression roller was also improved. In addition multi-layer printing with the updated machine was tested. This thesis focuses on the general design of the updated system and the measurement of key components of the systems as well as the print quality. Results demonstrate that the flat stamp can achieve the flatness of $\pm 16\mu\text{m}$ with thickness of $1194\mu\text{m}$; that the wrapping process can guarantee a print roller roundness error in the $20\mu\text{m}$ range; that the distortion of the print using the updated system is approximately 3.8. The multi-layer printing test did not achieve acceptable results owing to a lack of proper control of the machine. However, initial trials, achieved alignment errors of $1017\mu\text{m}$ along the printing direction and $113\mu\text{m}$ across the printing direction.

Thesis Supervisor: Dr. David E. Hardt
Title: Professor of Mechanical Engineering

ACKNOWLEDGEMENTS

First, thanks to my great teammates: Yufei Zhu, Paolo Baldesi and Charudatta Datar. We worked as a team on this project; their bright ideas and hard working help this project succeeds. Every one of them has their own specialties and strength that help me to learn not only in the project level but in many extended areas.

Many thanks to my advisor Professor Hardt, who gave us tremendous guidance and insights throughout the project. Meetings with Prof. Hardt were always enjoyable and enlightening.

I am also very gratitude to our supervisors in Nano Terra: Igor Sokolik, Werner Menzi, Brian Mayers, and Shih-chi Chen. Their resources and wealth of knowledge in the science of nano-manufacturing has been invaluable and has contributed greatly to our work.

Last but not the least, I want to thank my families for their encouragement and firm support in every aspects of my life.

Table of Content

Abstract	3
ACKNOWLEDGEMENTS	4
Table of Content	2
1 Introduction	7
1.1 Motivation.....	7
1.2 Problem Statement	8
1.3 Primary Analysis	9
1.4 Scope.....	10
1.5 Task Division	10
2 Literature Review	11
2.1 Soft Lithography.....	11
2.2 Micro-contact Printing	13
2.3 Existing Roll-to-Roll Equipment.....	14
2.4 Stamp Casting Machine.....	16
2.5 PDMS Peeling Process	18
2.5.1 Stress Zones at PDMS Peel-Front	18
2.5.2 Initiating Peeling.....	19
2.6 Printing Pressure	19
2.7 Multi-Layer Printing	22
2.8 Optical Methodology System Review	24
2.8.1 Laser Triangulation Sensors	24
2.8.2 Interferometer Sensors.....	26
2.8.3 Fiber Optic Sensors	27
2.8.4 Con-Focal Laser Scanning Microscopy.....	29
3 Methodology	32
3.1 Stamp Casting Machine.....	32
3.2 Peeling and Wrapping the Stamp on the Print Roller	34
3.2.1 Gripping the Film for Peeling.....	34
3.2.2 Methods to Generate Adhesive Force Between Backing Plate and Print Roller.....	36
3.2.3 Methods to Wrap Backing Plate without Loosing Alignment	37
3.2.4 Analysis of Fixture System.....	37
3.3 Precision Measurement Method	38
3.3.1 Flatness and Roundness Measurement	38
3.3.2 Distortion Measurement	41
3.3.3 Measurement of the Accuracy of the Alignment	44

4	Final Design: Results and Discussion	45
4.1	Flat Stamp Fabrication	45
4.1.1	Updated Flat Stamp Fabrication Device	45
4.1.2	Measurement of Flat Stamp Fabrication	48
4.2	Wrapping Flat Stamp onto The Print Roller	55
4.2.1	Updated Wrapping System	55
4.2.2	Measurement of Wrapping Quality	56
4.3	Single Layer Printing with Updated R2R Machine	58
4.3.1	Introduction of the Updated R2R Machine	58
4.3.2	Print Quality and Comparison with Previous R2R System.....	60
4.4	Multi-layer Printing with Updated R2R System	65
4.4.1	Introduction of Multi-Layer Printing Process	65
4.4.2	Measurement of Print quality	68
5	Summary and Future Work.....	72
6	Reference.....	74

Table of Figures

Figure 1: Illustration of the self-assembly process ^[2]	12
Figure 2: Steps Involved in Micro-Contact Printing ^[3]	13
Figure 3: Concept of the Machine ^[4]	14
Figure 4: Layout of The Three Modules in The Equipment ^[4]	15
Figure 5: The R2R Machine Built in '08 ^[4]	16
Figure 6: Main Parts of Aluminum Casting Machine for Large Area Stamp, Developed by Nano-Terra LLC.	17
Figure 7: Illustration of separation at the PDMS-Silicon wafer boundary ^[22]	19
Figure 8: Directions of peeling force ^[22]	19
Figure 9: Exploded view of impression Assembly and Bill of Materials ^[4]	20
Figure 10: Image of Different Load From Impression Roller ^[4]	21
Figure 11: Gravure Printing Machine.....	23
Figure 12: Actuation Method For Adjusting The Relative Distance Between Print Nips on The Substrate.	23
Figure 13: Simplified Sensing Method For Detecting The Relative Position Between Two Layers of Print in Gravure Printing.....	24
Figure 14: Principal of Laser Triangulation Sensor ^[14]	25
Figure 15: Principal of Interferometer System ^[15]	26
Figure 16: Total Internal Reflection inside Optical Fiber. ^[25]	28
Figure 17: Fiber Optic Probe Configuration ^[17]	28
Figure 18: Fiber Optic Probe Response Curve ^[17]	29
Figure 19: Principal of Con-Focal Microscopy ^[23]	30
Figure 20: Structure for Wafer Chuck.....	32
Figure 21: Teflon Spacer.....	33

Figure 22: Sidebars Used to Align Both Chucks.....	34
Figure 23: Illustration of Pint Roller Setup Before Wrapping.....	35
Figure 24: Illustration of the Proposed Fixture System.....	38
Figure 25: Fixtures for Flatness and Roundness Measurement	39
Figure 26: VERITAS VM 250	40
Figure 27: Measurement Setting for Roundness Measurement.....	41
Figure 28: The Shape of Rectangular- like Pixel.....	42
Figure 29: The Shape of Triangular Pixel	42
Figure 30: The Array of Two Kinds of Pixels.....	42
Figure 31: Demonstration of the Distortion	43
Figure 32: Pixel Dimensions ^[20]	43
Figure 33: Displacement of Two Printed Layers.....	44
Figure 34: 3D Model of Wafer Chuck for 12” wafer	46
Figure 35: 3D Model of Adapter of SS Chuck for 200mmx200mm Stamp Fabrication.....	47
Figure 36: 3D Model of Assembly for 12” wafer.....	47
Figure 37: Aluminum Vacuum Chuck Used in Last Year’s Project.....	48
Figure 38: Stainless Steel Vacuum Chuck Designed and Machined This Year	49
Figure 39: Using VERITAS 250 to measure the flatness of the vacuum chuck.....	49
Figure 40: Topographic Mapping of the Previous Vacuum Chuck	50
Figure 41: Topographic Mapping of New Vacuum Chuck	50
Figure 42: QQplot of The Test Result of The Previous Vacuum Chuck.....	51
Figure 43: QQplot of The Test Result of The new Vacuum Chuck	51
Figure 44: Histogram of The New Vacuum Chuck Test Result.....	52
Figure 45: Topographic Mapping of The Stamp Fabricated Using Last Year’s Device	53
Figure 46: Topographic Mapping of The Stamp Fabricated Using New Device	53

Figure 47: QQPlot of The Test Result for The Stamp Fabricated Using New Device	54
Figure 48: The Assemble Sequence of the SS Sheet	56
Figure 49: Different Print Roller used in 2008 (a) and 2009 (b)	57
Figure 50: Roundness Test Result of Previous Wrapping Method.....	58
Figure 51: Structure of the Flexure (Front View) ^[26]	59
Figure 52: The Updated Precision Shaft.....	60
Figure 53: The updated Linear Ball Bearing	60
Figure 54: Comparison of Tapered Contact Areas Using Previous and Updated Print System	61
Figure 55: Setup for The Repeatability of the Parallelism Test.....	62
Figure 56: Test Result of the Repeatability of Parallelism for Previous Impression Roller System.....	62
Figure 57: Test Result of the Repeatability of Parallelism for Updated Impression Roller System.....	63
Figure 58: Distortion Along and Across the Printing Direction	64
Figure 59: Diamond Pattern of Pixel Distortion in Last Year's Project	65
Figure 60: Position of Patterns After First Layer Printing.....	66
Figure 61: Position Alignment of the First Layer.....	66
Figure 62: Using Microscope to Align the Position of the Substrate	67
Figure 63: Adjustment of Second Layer printing	68
Figure 64: Multi-Layer Printing Result	69
Figure 65: Relative Position of Two Layers.....	69
Figure 66: Microscope Used for Multi-Layer Printing.....	70

1 Introduction

1.1 Motivation

Currently, nanostructures are commonly fabricated using techniques such as photolithography, electron-beam writing and X-ray lithography. Although these methods are proven technologies that provide high-quality outputs, there are inherent problems. These techniques are generally expensive, slow, and the production of large patterns is difficult. Micro-contact printing (μ CP) is a promising technology in which a patterned elastomeric stamp is used to transfer patterns of self-assembled monolayer (SAMs) onto a substrate by conformal contact printing. In 2008, a group of MIT students developed a high throughput, low cost roll-to-roll (R2R) printing technique into micro-contact printing, achieving good results. They also built a prototype machine to realize the whole process in the speed of 400 feet per minute while maintaining good quality outputs.

However, the last year's machine is only limited to printing octadecanethiols, an organic ink, on gold substrates where the self-assembly characteristics (see section 2.1) of these media could tolerate big range of pressure variance applied on the substrate. Therefore, if the micro-contact printing is applied into some other media where self-assembly characteristics do not exist, a highly uniform pressure along the substrate will be critical to the quality of outputs. The pressure of previous prototype machine is provided by the contact of the print roller and the impression roller. The uniform roundness and straightness of the rollers is key to the uniform pressure along the contact area. Meanwhile the parallel contact between the impression roller and the printer roller is also very important. Therefore, if we can fabricate the print roller with the variance less than a few microns and the contact between the impression roller and the printer roller has good parallelism with high repeatability, then the roll-to-roll micro-contact printing technology could be easily applied to various printing media.

The printer roller consists of central shaft, sleeve, the backing plate and the stamp (see section 2.2). The uniform thickness of the stamp is the most critical component of the uniform roundness of the print roller. Currently, there is no standard process to fabricate the stamp with the thickness variance of a few microns, therefore, the repeatable, reliable and manufacturable stamp fabrication process is also highly desired.

Another limitation of last year's project is that the registration of multiple layers on a flying substrate was not considered; only monolayer could be printed using the prototype machine. However, in the industry, multi-layer printing is required, which means to print another layer on the substrate with patterns. At present, the commercial printing industry, where multi-layer printing is very common and popular, can only achieve a resolution of 40 microns. Thus, such technology can hardly be applied to multi-layer printing where the pixel size is less than 40

microns. If multi-layer printing with the resolution of 1 micron could be demonstrated by upgrading the previous prototype machine, there will be a significant impact in the printing industry.

Research was funded by and in cooperation with Nano Terra Inc, a Cambridge, Massachusetts company that specializes in Soft Lithography.

1.2 Problem Statement

The primary objective of this project is to address the limitations of the previous prototype machine in related to the potential manufacturing of printed electronics using micro-contact printing technique within the soft lithography (SL) field.

At first glance, the main goals of this project can be split in two major areas:

Improve the printing quality, upgrading the R2R system built by the MIT students in 2008; in particular this goal will be achieved by designing and fabricating an interchangeable stamp on the roller that allows a quick replacement of the stamp once it is used up, without losing of alignment. This goal is achieved by performing four key steps:

- Design of an interchangeable stamp
- Fabrication and demonstration of interchangeable stamp
- Test results providing data on distortion, alignment
- Budget estimate for manufacturing applications

The second main goal of the project is to improve the overall R2R system. This task is achieved by executing the following steps:

- Redesigning and implementing the impression roller system
- Designing process for multi-layer printing
- Designing high precision positioning system for the print roller adjustment
- Test results providing data on distortion and alignment
- Budget estimate for manufacturing applications

1.3 Primary Analysis

We considered the two major goals of the project, namely, fabricating a very flat stamp and then wrapping it around the print roller, and proving that micro-contact printing can be used for printing multiple layers with alignment.

In order to fulfill these goals, our approach consisted of accomplishing the followings:

1. Flat stamp fabrication. To achieve this, a new method was developed to fabricate the stamp using a molding process, to ensure a flat and defect-free stamp.
2. Wrapping the stamp with backing plate onto the roller with alignment and repeatability. The goals of this process were to wrap the stamp while maintaining alignment, and developing a repeatable process; and to maintain uniform roundness of the stamp after wrapping. To achieve this, after looking at a lot of options, we decided to use a magnetic cylinder, and a pin-slot system to grab the edge of the backing plate. We also considered a fixture system to wrap the stamp with backing plate on the cylinder.
3. Ensuring the roundness of assembled print roller within 4 microns tolerance. With proper wrapping method, minimal and uniform printing pressure could be achieved and hence realized good printing quality.
4. Redesigning the impression roller system to improve its repeatability of parallelism. In this process, we built up error budget model, found out the constraint to the repeatability of the impression roller system and then updated the system.
5. Designing a high precision position system to control the print roller position and orientation. This step was fundamental to improve the quality of single layer printing as well as the multiple layers printing.
6. Printing using the updated machine and comparing results that achieved by last year's group. After we qualified the wrapped stamp and impression roller system, we mounted the new roller onto the current machine, to get a direct comparison of print quality.
7. Printing multiple layers as a proof of concept. This was an independent step, to prove that micro-contact printing can print multiple layers on a single substrate with minimum misalignment.

1.4 Scope

Our project only dealt with micro-contact printing with PDMS as the stamp and 300mm wafer as the master. We focused on printing thiol onto gold-coated substrates. This scope allowed us to decide the dimensions of our design based on available materials. The mature printing mechanism also allowed us to verify our designs without disturbance of different printing conditions.

For multi-layer printing, the initial purpose was to use rigid and transparent material (glass) as the substrate to print two layers using the same stamp to print twice. Later on, the scope switched to using updated R2R machine to print two layers with the same stamp in order to demonstrate what is the best alignment can be achieved using current Roll-to-Roll technology. In order to achieve this target, precise control of the printer roller on its alignment is required and we assumed the motion of the flexible substrate is self-aligned across the printing direction.

1.5 Task Division

This thesis is based on a team project executed as part of the Mechanical Engineering Master of Engineering in Manufacturing Degree Program. The team members were:

Wenzhuo Yang has researched and determined the measurement methods for cylinder roundness, tolerance of stamp fabrication parts as well as the print quality of output features. He designed the measurement structure and analyzed the data obtain from both measurements. In addition, he worked with Yufei Zhu on the upgrade of impression roller system and multi-layer printing process design.

Paolo Baldesi has designed the high precision positioning system to control the position of the print roller. He calibrated the system and determined its performance. In addition, he worked with Charudatta Datar in developing an innovative wrapping process designing a new magnetic print roller. He also researched and designed the mechanism of growing UV-curable material onto cylinder directly.

Charudatta Datar has designed the magnetic roller, and developed the technique to attach and wrap the backing plate and PDMS stamp onto the print roller. He also worked with Paolo Baldesi in designing the high precision positioning system. In addition, he designed other components, compatible the high precision positioning system, to mount the new print roller on the machine built by the MIT '08 team.

Yufei Zhu designed prototype machine for the multi-layer printing for rigid substrates. He also designed the stamp fabrication parts with Mr. Werner Mezi from Nano-terra Inc.

We collectively tested the machine and determined the quality of printing resulted from the machines. Since we were working on a common project, the first three Chapters of our individual theses are common.

2 Literature Review

This section summarizes the existing R2R machine developed in 2008 by Adam Stagnaro, Kanika Khanna, and Xiao Shen ^[4,20,21], introduced the technologies used in the machine, and described its structure, function, operation steps and the result achieved. Also some pioneering studies of the currently multi-layer printing technology were reviewed to enlighten our prototype design on current R2R machine. Finally, some popular and representative optical metrology systems are studied to search out proper methods for measuring the quality of the machine design and the print output.

2.1 Soft Lithography

Photolithography is a well-established micro-fabrication technology, being widely used to manufacture most integrated circuits. It is, however, limited to a feature size of about 100 nm owing to optical limitations. Technologies such as extreme UV lithography, soft X-ray lithography, electron-beam writing, focused ion beam writing, and proximal-probe lithography^[1] are capable of manufacturing smaller features, however, they are limited by high cost and technology development.

Photolithography also has other limitations: it cannot be used on non-planar surfaces; it is incapable of producing three-dimensional structures, and it is not suitable for generating patterns on glass, plastics, ceramics, or carbon ^[1].

Thus, a family of techniques called as soft lithography, including, microcontact printing, replica molding (REM), microtransfer molding (mTM), micromolding in capillaries (MIMIC), and solvent-assisted micromolding (SAMIM) are emerging as prospective solutions to overcome some of the limitations of photolithography.

They offer a number of basic advantages, such as, little capital investment, and simplicity. Apart from these, soft lithography techniques can produce features smaller than 100 nm, with relatively simple technology, and they are not subject to optical limitations. They also offer flexibility in terms of surface material, and shape, overcoming some of photolithographic limitations.

These techniques are referred to as “soft lithography” because each technique makes use of flexible organic materials as opposed to rigid materials to achieve pattern transfer to the substrate. Basically, these techniques involve the fabrication of an elastomeric stamp (typically made of Polydimethylsiloxane, PDMS), generating a replica of the pattern originally on a Silicon master, and using this stamp to print the pattern on a substrate using self-assembly.

Self-assembly refers to the spontaneous formation of molecules into organized structures by non-covalent forces. The resulting structure is highly uniform, defect-free owing to thermal

equilibrium, and in the lowest energy form.

Self-assembled monolayer (SAM) is one such non-biological self-assembly system (see figure 1 for its process). SAMs is used in soft lithography to transfer the pattern on the elastomeric stamp, onto the surface of the substrate using minimal contact pressure.

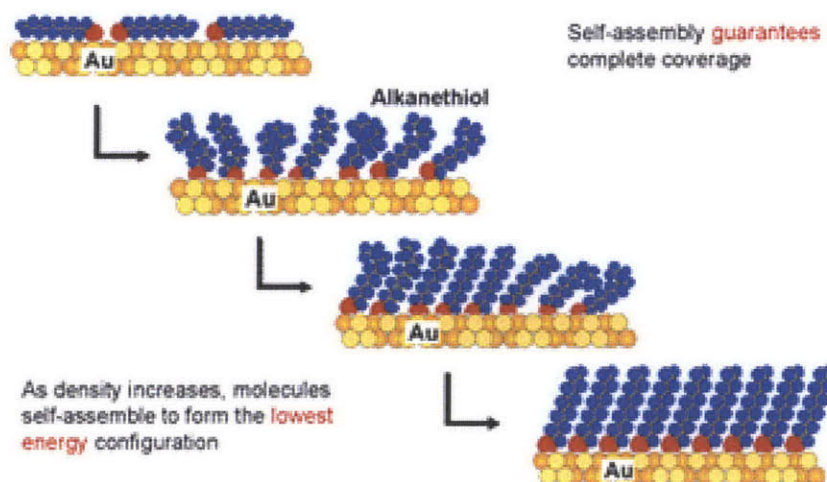


Figure 1: Illustration of the self-assembly process ^[2]

We lay emphasis upon one of soft lithography techniques, micro-contact printing, because we used this method throughout the project. This paper does not describe the other methods.

2.2 Micro-contact Printing

The micro-contact printing process involves transferring a pattern on an elastomeric stamp onto the surface of a substrate by the formation of a monolayer of ink, which can be used as resist in subsequent etching, or other steps. This process relies on SAM, in which it enables transfer of only a monolayer of ink to the substrate. This molecular level contact makes the process independent of excessive ink being trapped between stamp and substrate, allowing significantly smaller sized (~ 50 nm) features to be printed onto the substrate.

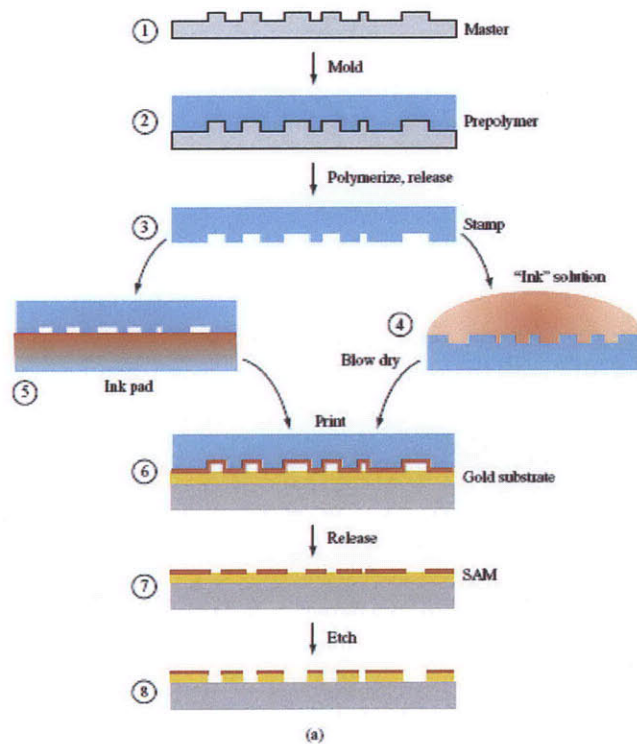


Figure 2: Steps Involved in Micro-Contact Printing ^[3]

The micro-contact printing process, as shown in figure 2, involves, like all soft lithography techniques:

1. A master with the original pattern on it. This is typically a patterned Silicon wafer.
2. This pattern is then replicated on a PDMS stamp by casting or molding.
3. This PDMS stamp is then inked, by a couple of methods (using an ink pad, or pouring ink over the stamp).

4. Next, this inked stamp comes into contact with the substrate that is to be printed upon.
5. This contact enables the formation of a SAM of the ink on the surface of the substrate.
6. The stamp is released, and the SAM formed on the substrate is then used in subsequent etching steps to generate the required pattern on the substrate.

2.3 Existing Roll-to-Roll Equipment

The MIT'08 team's (Adam Stagnaro, Kanika Khanna, and Xiao Shen^[4,20,21]) task was to take this demonstration to the next level, and prove that the paradigm would be competitive with commercial printing systems in at least one of the parameters - quality, rate, flexibility.

The key goal of this MIT'08 project was to achieve Micro-contact printing at very high speeds (400 ft/min), on 8" wide coated substrate (web).

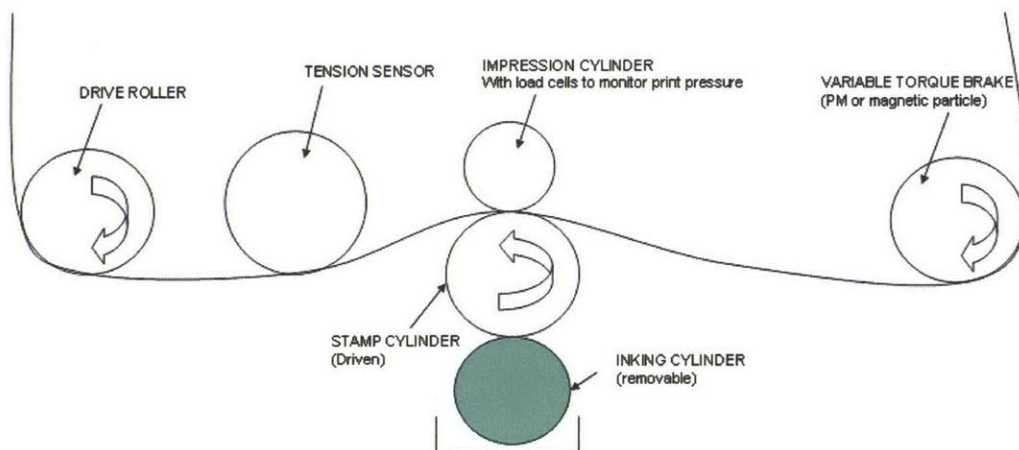


Figure 3: Concept of the Machine^[4]

The concept of the machine is shown in figure 3. The substrate was in the form of a web, driven through a set of rolls. A combination of open and closed loop using motors and clutches was used to achieve tension control.

The equipment can be divided into three modules:

1. Supply Module (to unwind substrate web),
2. Print Module (to ink, print, and apply pressure), and
3. Collect Module (to rewind substrate web)^[4]

Figure 4 shows the layout of the machine, in terms of these three modules. The entire roller system is cantilevered about a common base plate. And figure 5 shows the physical appearance of the R2R machine built by 08' group.

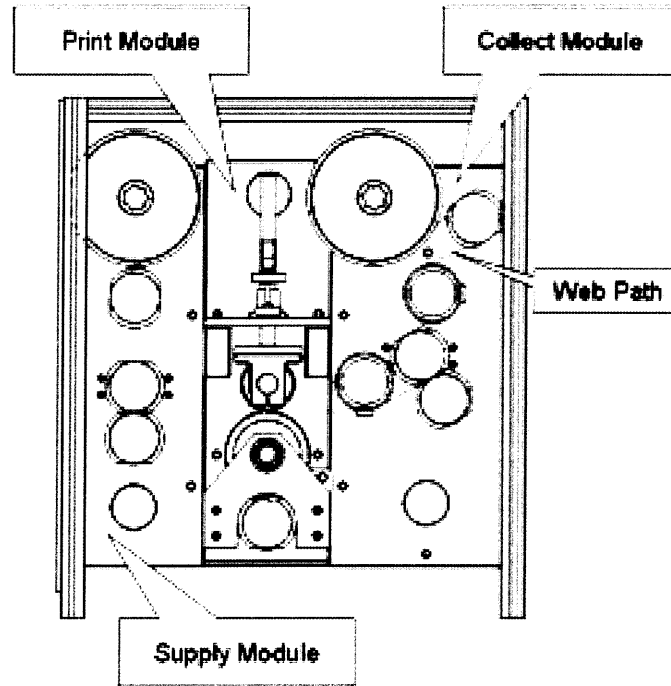


Figure 4: Layout of The Three Modules in The Equipment ^[4]

We shall not describe the operation of the machine in much detail, but will emphasize on the results of the print module only, as this was felt to have the most significant impact on the results, which also have been described in detail later in this document.

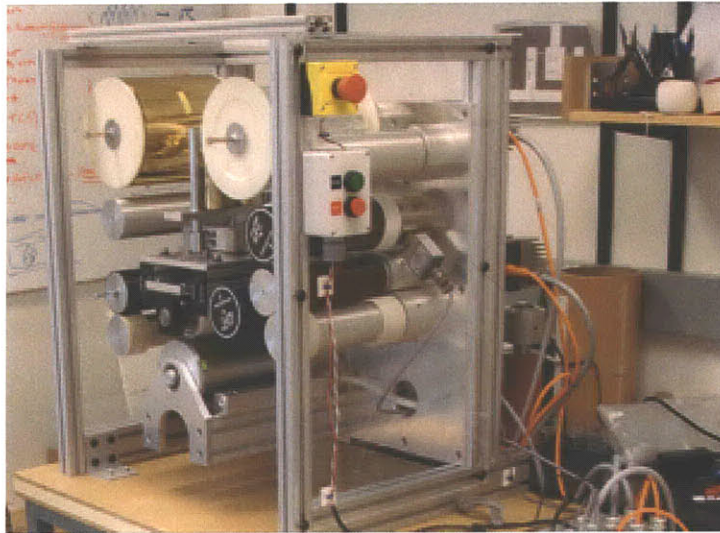


Figure 5: The R2R Machine Built in '08 ^[4]

A series of experiments were designed and conducted to test the printing quality. Below is a summary of relevant results ^[4].

1. Neither printing pressure nor speed was found to have a significant effect on spatial distortions and pattern dimensions in the range of settings we used.
2. It is possible to print a robust etch-resisting SAM at very high speeds (400 ft/min, unit area contact time ~ 5 ms).
3. At very high speeds (400ft/min), some systematic air trapping was observed
4. The alignment of the stamp on the backing may have a significant effect on distortion patterns.

These results have formed the basis for our project. Improvements in the following were seen as critical to improving the printing quality:

1. Alignment of the stamp on the backing, and therefore on the print roller
2. Fabrication of a flat stamp
3. Precision in the web handling system of the equipment

2.4 Stamp Casting Machine

Stamp fabrication is essential to improve the quality of printing. Micro-contact printing requires precise transfer of patterns with minimum distortion and maximum yield. In addition, the stamp needs to maintain an exactly complementary pattern to the master, and it should avoid distortion during printing.

PDMS as the material for stamp has a low Young's modulus; therefore, under tension or external force, the PDMS will distort and result in a distorted pattern. In previous projects, PDMS has been cast onto a rigid backing plate. The backing plate is treated with a plasma and surface treatment chemicals to increase its adhesion to PDMS, and the force between this backing plate and PDMS is firm enough that little relative motion between the stamp and backing plate will happen. Thus, the backing plate with PDMS minimizes distortion when wrapping the stamp onto the print roller.

With the consideration of cost and efficiency, large stamps are desired for production. In common practice, round wafers (150mm, 200mm and 300mm size) are used as the master and etched out negative pattern on the SU-8 layer on the master. This photo-resist will directly contact PDMS during the practice, thus caution should be made in order not to destroy the pattern on the master. The size of the stamp is limited by the size of wafer. In this project we targeted 300mm wafer as our master and explored the problems including distortion, uniformity, peeling force from master and repeatability with the capability of scaling in manufacturing.

In previous research at Nano-Terra LLC, the thickness of the stamp was shown to affect the pattern transfer and a thin stamp seems to result in better printing quality. This research is not restricted to self-assembly monolayer printing, for applications in which pressure is critical to the quality and yield of printing, the elasticity property of the stamp will be a key consideration and this property is directly affected by the thickness of stamp. A uniform, thin layer of stamp is beneficial to other on-going projects in the soft lithography.

Nano-Terra developed their first casting machine (see Figure 6) using aluminum with a 12" master, which demonstrated capability of large area stamp fabrication. In figure 6, a vacuum chuck at the left holds the backing plate and flips onto the wafer chuck at the right where the wafer sits. PDMS is injected into the gap between the backing plate and wafer.

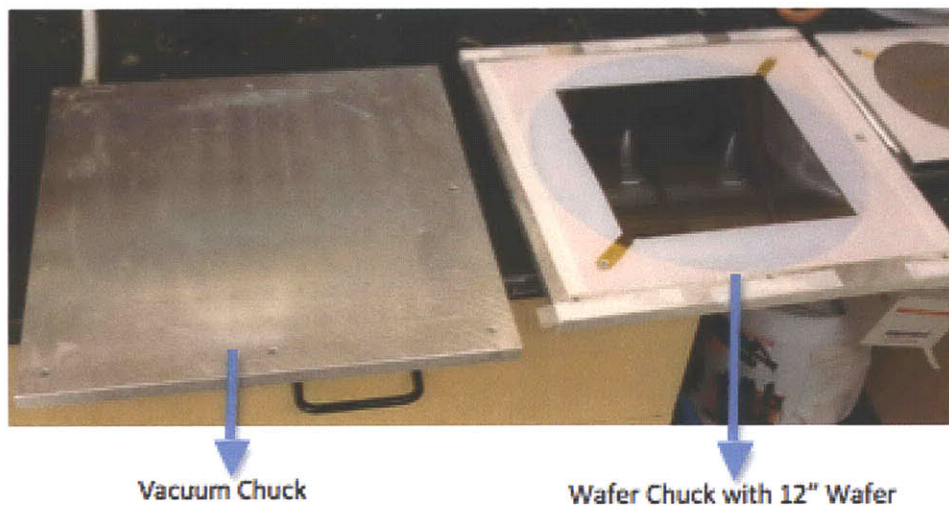


Figure 6: Main Parts of Aluminum Casting Machine for Large Area Stamp, Developed by Nano-Terra LLC.

As shown in figure 6, this configuration is to have two vacuum chucks : one attaching the master and the other attaching the backing plate. A dam (or reservoir) is placed around the area. These two chucks face each other, and create a space, which is circled by the dam. Liquid PDMS is injected into the area with a syringe.

This pilot stamp fabrication equipment demonstrated consistent quality for use in large size stamp. However it is not designed for interchangeable masters because its mechanism for fixing the master does not allow quick uninstal. Also the space between backing and can't be adjusted easily. Thus it was not able to experiment for manufacturing purpose. Surface finish of the vacuum chuck is rough, which results in uniformed thickness across the stamp.

To resolve these problems identified from this pilot PDMS casting machine, a better material that is capable of ultra-high precision machining is necessary. The Wafer chuck will be modified to add-in alignment capability for maintaining repeatability each time a new master is brought in. Thickness of stamp can be varied by changing the spacing part between wafer and backing plate. This is the topic of Yufei Zhu's thesis ^[24], detail explanation on stamp fabrication process could be found in his thesis.

2.5 PDMS Peeling Process

The peeling process is a crucial step where we need to wrap a PDM stamp, which initially lies flat on a Silicon wafer, onto the print roller. Thus, it is essential to first successfully peel the PDMS stamp without any tears or distortions. This section studies some of the research that has been done on peeling PDMS off Silicon wafer.

2.5.1 Stress Zones at PDMS Peel-Front

Considerable research has been done on peeling PDMS off a Silicon wafer. However, the upper side of PDMS is not attached to any other surface (like a metal plate), but is open to air. In our project, the topside of PDMS is attached to a steel backing plate. However, some of the findings of the research are indeed useful despite this difference, and are as below.

In general, at the peel front, boundary conditions are different on the two sides of the PDMS stamp; in fact, on one side, the surface of the film has zero shear stress (or very small shear stress, in our case) because it is not attached any surface (or to a different surface), while on the other side, the film adheres to the silicon master and shear stress is imposed on it by the substrate. This configuration creates a singularity around the peel front. This very small and thin zone is characterized by a highly variable stress values. This stress singularity in the normal direction causes the separation of the film at the peel-front.

When viewed closely to the peel front, peeling of PDMS could be schematized as below:

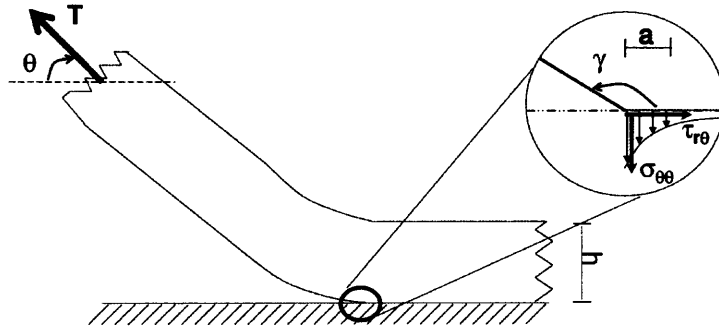


Figure 7: Illustration of separation at the PDMS-Silicon wafer boundary ^[22]

2.5.2 Initiating Peeling

Generally, to initiate the peeling operation we need apply a force at the peeling front, and as shown in figure 8, this force can be applied either, A: an upward force on the top surface of the film or B: a force applied at the edge on the bottom surface.

Previous works showed that, the success of either approach depends on how close the applied force is to the vertical plane of the peel-front. Only when the force is applied in the same vertical plane as the edge, the singularity at the edge results in peel-initiation.

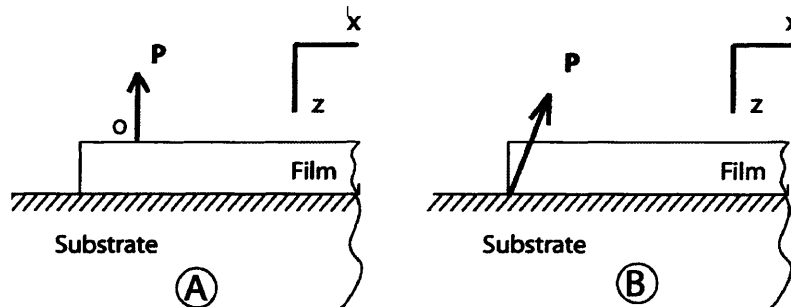


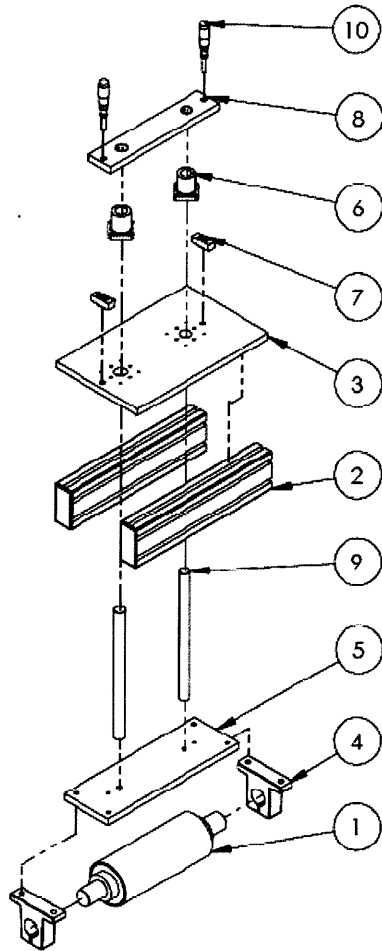
Figure 8: Directions of peeling force ^[22]

2.6 Printing Pressure

Since the scope of Nano-Terra 2008 group was limited to monolayer printing using SAM as the conformal printing surface, pressure has low effect on the printing quality. The experiments carried out in 2008 indicate that when printing pressure falls in the range of 15.88kPa to

41.14kPa, or within overall load of 3.5lbs to 26.8lbs, quality of printing is not affected by change of pressure ^[4]. Because of this character of SAM, the design did not require high precision on the printing area.

Since the machine is designed with three main modules, each module has minimal interaction, thus allowing module upgrade for different purposes. As mentioned before it was built to test the highest achievable throughput using the micron-contact printing technology.



ITEM NO.	DESCRIPTION	QTY.
1	IDLER ROLLER ASSY	1
2	8020 STANDOFF	2
3	IMPRESSION FIXED PLATE	1
4	SHAFT MOUNT	2
5	SHAFT SUPPORT PLATE	1
6	LINEAR BALL BEARING	2
7	LOAD CELL	2
8	PRESSURE PLATE	1
9	LINEAR SHAFT, .750"	2
10	MICROMETER	2

Figure 9: Exploded view of impression Assembly and Bill of Materials ^[4].

We focused on improving the impression module at the center of this machine (see figure 9 for the explosive view of impression roller system). The Impression Roller Assembly will be replaced (Item #5). The goal of this improvement is to increase the repeatability of web position as well as web path. We also brought pressure sensor into the machine, enabling pressure adjustment for this machine. All these new improvements are beneficial for future applications other than self-assembly printing. These applications require better pressure control as well as

repeatability during printing. We also expected to make the machine more accurate in web handling and the print roller adjustment, both of which are the foundation for multi-layer printing.

In previous project the pressure as printing parameter has been tested. The experiments were carried out by loading impression roller onto a stationary inked printing roller with a strip of substrate in between. Thus the developed patterns after represent the actual contact area between impression roller and printing roller. Because the alignment is not easy to achieve in the print roller, the impression roller and print roller are not parallel and the contact area is tapered, as shown in figure 10.

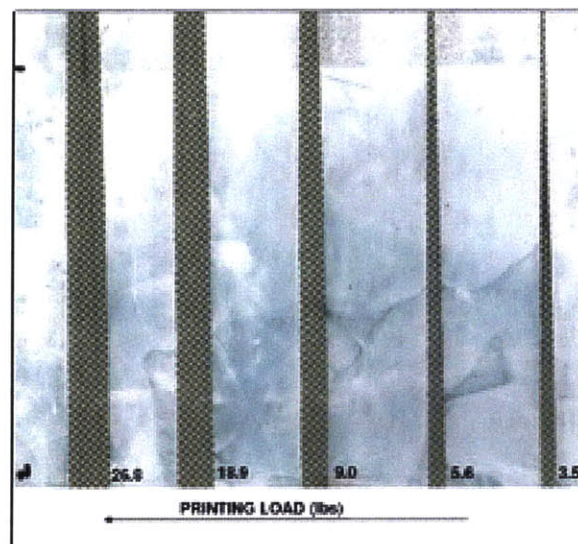


Figure 10: Image of Different Load From Impression Roller ^[4].

To investigate the reasons for non-parallel contact, an error budge was carefully studied. As show in table 1, the built-up error of all these components is small compared to error introduced by weight. Under 3.5 pound pressure, the right stripe in figure 12 has top width as 0.09 inch, and bottom width as 0.23 inch^[4].

Table 1 List of Parts in Impression Assembly

Item	Description	Qty	Manufacturer	Vendor	Part #	Error
1	MODULE PLATE, PRINT	1	NT-MIT	MD Belanger	P101	0.075mm/40cm
2	SHAFT SUPPORT PLATE	1	NT-MIT	MD Belanger	P114	0.075mm/40cm
3	IMPRESSION FIXED PLATE	1	NT-MIT	MD Belanger	P116	0.075mm/40cm
4	IDLER ROLLER ASSY	1	DFE	DFE	IR3-8-45	N/A
5	LINEAR BEARING ASSY	2	THOMSON	M-C	64825K36	N/A
6	LINEAR SHAFT, .750"	2	THOMSON	M-C	6649K61	0.002"/12"
7	SHAFT MOUNT	2		M-C	6068K27	N/A
8	8020 STAND OFF	2		8020		N/A

2.7 Multi-Layer Printing

After the successful demonstration of high throughput and good yield in one-layer printing using R2R machine, our background knowledge is sufficient to start the research in micro-contact printing's capability of multi-layer printing. This is an important step towards the actual application in manufacturing because micro-contact printing is no longer limited to printing of photo-resistive material as the ink. Further applications require multiple layers to overlap to achieve complex function. The units under consideration include diodes and transistors with at least 3 layers.

An important specification introduced in multi-layer printing is accuracy in relative layer position or registration. We are expecting to achieve registration with the roll-to-roll structure, because of the high throughput. However most literature discusses methods to align surface to surface, including the alignment between mask and wafer in semiconductor industry, or dip and substrate in inkjet printing, while few have mentioned alignment issue between round subject and flat substrate. Thus references for designing machine capable of multi-layer printing will be mainly from color printing industry.

It is common practice to start building high precision system based on an open-loop structure and to add-in close loop component to increase the accuracy. An open-loop structure is simple because micro-contact printing requires only two motions: linear motion of substrate and rotational motion of the print roller. Since roll-to-roll machines are widely used in printing industry, it is beneficial to learn how the feedback systems work. We will use gravure printing to demonstrate how the printing industry achieves this registration. Figure 11 shows a typical gravure-printing machine.



Figure 11: Gravure Printing Machine.

Gravure is widely used in high quality printing. Because human eyes are not sensitive to features less than 40 micron wide, the feedback system for gravure machines usually set the accuracy at 100 micron or less. Errors in two key directions have been compensated. One is the direction of substrate motion during printing, or the “path”; the other is the direction perpendicular to the path on substrate plate. The latter is easy to adjust by moving roller along its axis; the error in path is sensed and compensated using sleeve displacement between the roller and the sleeve (see figure 12).

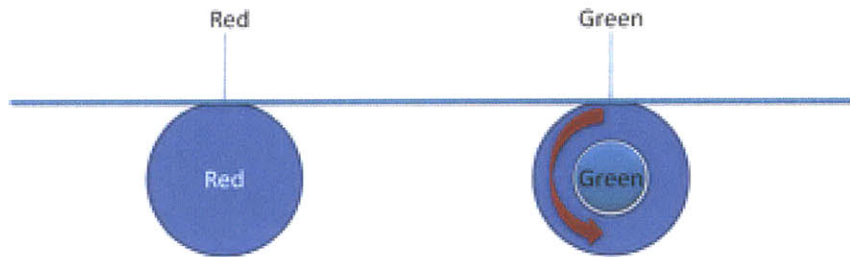


Figure 12: Actuation Method For Adjusting The Relative Distance Between Print Nips on The Substrate.

In Gravure printing, marks are printed with a distance of 20mm, and individual roller prints each color mark. Sensors are used to check the distance between marks to determine the relative position between different colors on substrate. The sensor system is shown in figure 13. The signal from sensors are received only when designated color are about to arrive. Once an error is detected, the controller will send out signals to the roller whose color is offset from its desired position, and the sleeve on the roller will rotate to compensate for this error.

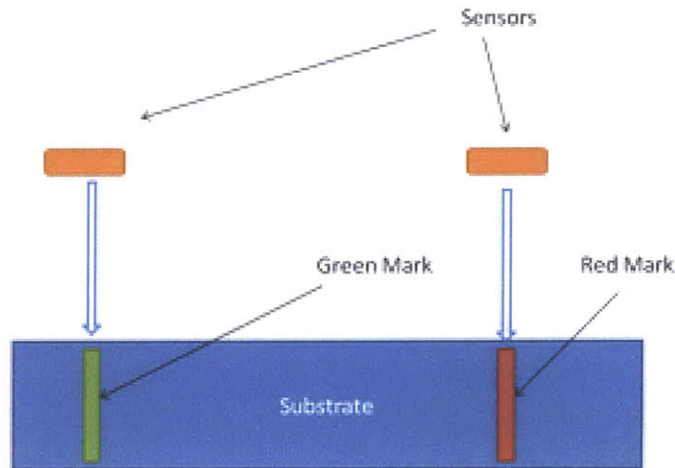


Figure 13: Simplified Sensing Method For Detecting The Relative Position Between Two Layers of Print in Gravure Printing.

Assume both red and green rollers are rolling at the same speed, the green and red mark on the substrate will have a constant distance of 20mm, and signals from both sensors will reach controller at the same time. If, however the green roller is one step behind compared to the red roller, the green mark will shift back at some distance, and a signal from the green sensor will lag from the red signal. The controller will determine the amount of offset from the time of this lag and control the sleeve on green roller to shift one step ahead.

2.8 Optical Methodology System Review

One of the objectives of the project is to fabricate the stamp within the variance of $\pm 4\mu$, which means high precision measurement tools has to be employed. Currently, there are various kinds measurement sensors that can achieve very high accuracy and resolution, but they also have specifications that match some specific needs. In this section, laser triangulation sensors, interferometers, fiber optic sensors and con-focal microscopy are reviewed as our potential choice of measurement sensors.

2.8.1 Laser Triangulation Sensors

Triangulation measurement is an old but very useful method to measure distance. Laser sensor is a powerful tool, using triangulation measurement, to measure either long-distance or short-distance with high accuracy. However, the long distance measurement may not provide

very high resolution. Laser sensor projects a spot of light onto the target and receives the reflected light with photo detector through an optical lens. A typical laser triangulation system is shown in Figure 14 below.

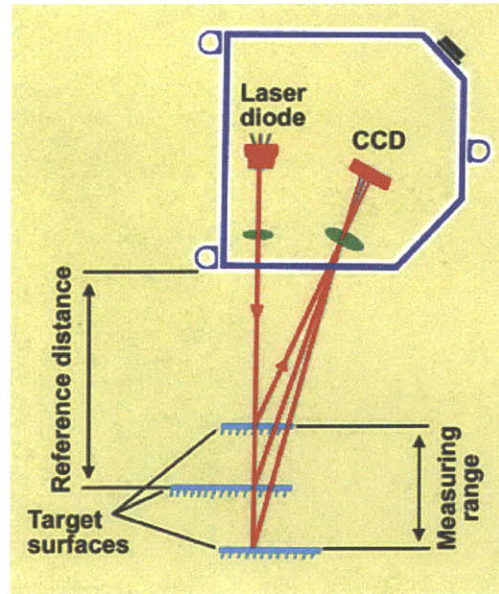


Figure 14: Principal of Laser Triangulation Sensor ^[14]

From the figure 14, we could see that the relative position of laser diode, lens, photo detector and the position of reflected light from the target on the photo detector determine the distance of the target. If the target changes its position, the reflected light changes its position on the photo detector as well. Through linearization and additional digital or analogue signal processing, the detector could provide an output signal proportional to the position of the target. The ambient light has little effect on reading, because the signal is proportional to the center of intensity of the focused image ^[14].

The most important part of a laser sensor is the photo detector, which could be a photo diode, position sensitive device (PSD), charge-coupled device (CCD), Complementary metal-oxide-semiconductor (CMOS), etc^[14]. Different photo detectors require different signal processing methods.

The following summary of general laser triangulation sensors' characteristics is built upon the works done by Alexander H. Slocum in his book named *Precision Machine Design* ^[16], updated with recent industry standards. Note that the manufacturers are always advancing the state-of-art, so this summary is a generalization only.

Size: Typically 30x50x70mm

Cost: Depends on the resolution. Normally, 1 μ resolution laser sensor cost \$4000.

Measurement Range (span): 3 - 1300mm

Accuracy (linearity): 0.03% of Span, 500 Hz, to white target (85% diffuse reflectance)

Repeatability: Depends on the repeatability of the surface finish.

Resolution: on the order of 0.005% of full-scale range, could achieve as high as 0.1μ

Laser spot size: 30-300 μ m

Environment Effect on Accuracy: On the order of 0.01%/°C of full-scale range from the nominal 20°C operating temperature

Power: 15 – 24 Volts DC, 120 – 200 mA draw with 350 mA surge at power-up

Allowable Operating Environment: Keep optical windows clean for best performance. System typically operate from 0 to 40 °C

2.8.2 Interferometer Sensors

Various kinds of interferometers are in use today. Michelson interferometer has the most common configuration for optical Interferometry and was invented by Albert Abraham Michelson. A typical and simplified interferometer system is shown schematically in Figure 15.

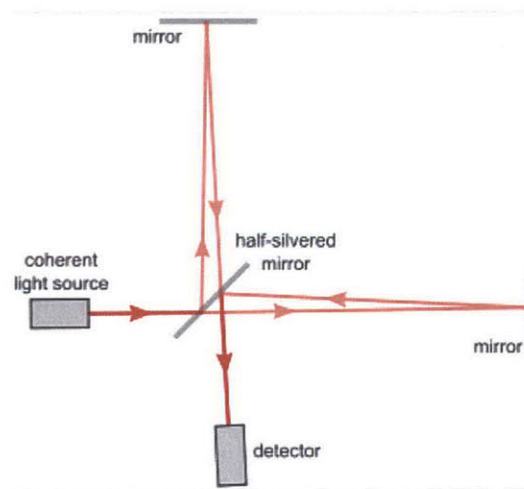


Figure 15: Principal of Interferometer System ^[15]

According to figure 18, a continuous light source was splitted into two paths: One bounces back from the semi-transparent mirror, and then reflects back from the mirror on the top, goes through

the semi-transparent mirror, to the detector. The other one goes through the semi-transparent mirror, bounces back from the mirror at right, and then reflects back by the same semi-transparent mirror and goes into the detector. Difference in path may result from the length difference or different materials, which cause alternating pattern on the detector. If no difference of materials involved in the interference, the distance could be measured through

The following summary of general laser triangulation sensors' characteristics is built upon the works done by Alexander H. Slocum in his book named *Precision Machine Design*^[16], updated with recent industry standards. Note that the manufacturers are always advancing the state-of-art, so this summary is generalization only. It is also extremely important to stress that the accuracy of measurement is highly depended to the manner of how the optics are mounted and how the environment are controlled.

Size: Laser head, 130x180x530mm.

Cost: About \$9000 for laser head and electronics boxes for up to 4 axes of measurement.

Measurement Range (span): up to 30m^[16]

Accuracy: In a vacuum, if perfectly aligned, the accuracy can be on the order of half (worse) the resolution. As for non-vacuum conditions, the environment significantly impacts the accuracy of measurement.

Repeatability: Depends on the stability of the environment and the laser head.

Resolution: Depends on optic used and can be achieved as high as $\lambda/4096$. Higher resolution could be achieved through better optics and phase measurement technique involved.

Environment Effect on Accuracy: About $1\mu\text{m}/\text{m}^{\circ}\text{C}$ Air turbulence and thermal expansion of optics, mounts and the machine itself^[16].

Power: 12 V, 200 mA (PICO M8 con.)

Allowable Operating Environment: Since the interferometer is sensitive to the environment, ideally, it should be used in a vacuum, or in air of 20°C with no gradients.

2.8.3 Fiber Optic Sensors

Optical fibers are glass or plastic fibers that transmit light using the property of total internal reflection and the fiber act as waveguide^[25]. Figure 16 demonstrates the total internal reflection of a laser inside the optical fiber.

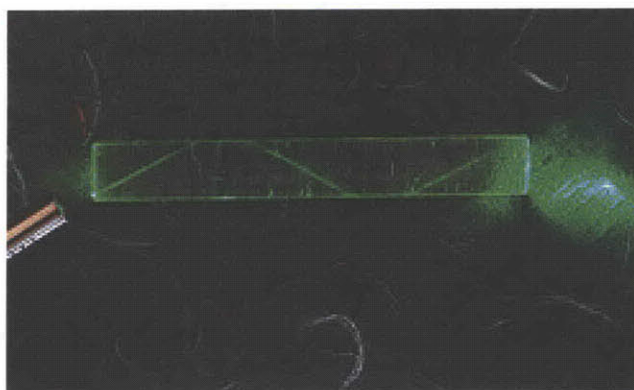


Figure 16: Total Internal Reflection inside Optical Fiber. ^[25]

The key elements for fiber optic sensor are two sets of flexible probes: one is for transmitting and the other is for receiving. Two probes are jacketed into one to measure the distance. There are basically three kinds of probes configurations: Hemisphere, Random and concentric, as shown in Figure 17. Active diameter of probes could be as small as 0.177mm, making them ideal to measure small target ^[17].

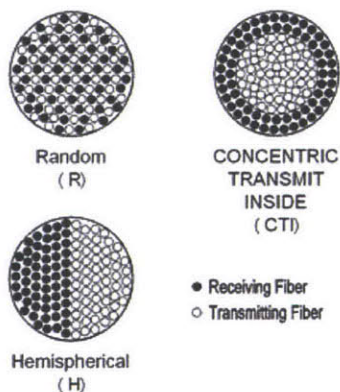


Figure 17: Fiber Optic Probe Configuration ^[17]

The distance of an object can be determined based on the intensity of reflected light that is sensed by two transmitting and receiving fiber probes ^[18]. The response curve is shown in Figure 18, and the intensity of reflected light is converted to voltage output. Optic Fibers are not sensitive to electromagnetic interference and typically very light ^[16].

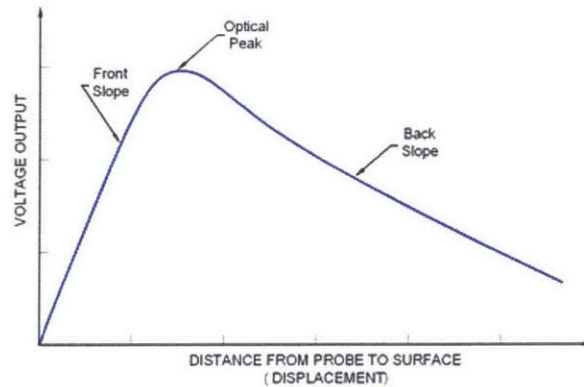


Figure 18: Fiber Optic Probe Response Curve ^[17]

The following summary of general laser triangulation sensors' characteristics is built upon the works done by Alexander H. Slocum in his book named *Precision Machine Design* ^[16], updated with recent industry standards. Note that the manufacturers are always advancing the state-of-art, so this summary is generalization only.

Size: cable diameter could be 1mm or even smaller

Cost: Depends on the type of sensor, \$100-\$1000.

Measurement Range (span): a few millimeters for small displacement (<10mm)

Accuracy: 0.1% of full range;

Repeatability: Depends on environment conditions

Resolution: Can achieve very high resolution if the sensor held very close to the target, like 0.01 μ m resolution with the range of 0.1mm

Environment Effect on Accuracy: very sensitive to environment, like dirt on the sensor will degrade the performance.

Allowable Operating Environment: Since the interferometer is sensitive to the environment, the sensing surface must be kept very clean. Individual probes should be kept away from moisture, or they will eventually erode to the point of failure.

2.8.4 Con-Focal Laser Scanning Microscopy

Con-focal laser scanning microscopy (CLSM or LSCM) is a technique that could capture very sharp optical images at selected height ^[23]. A very important feature of con-focal microscopy is

that it could obtain images from various depths. Because of its high resolution on depth measurement, the con-focal microscopy could be applied to measure the flatness of object within the limitation of the measurement tool.

In con-focal laser scanning microscopy, a coherent light source projects a beam of laser, which goes through the beam splitter and focused on the target via lens. Scattered and reflected laser light, together with the illumination light, were re-collected by the lens and then focus on the detector via the reflection of the same beam splitter. The aperture of detector blocks the light that is not from the focal point and hence leads to a sharper image comparing to conventional microscopy. (See figure 19)

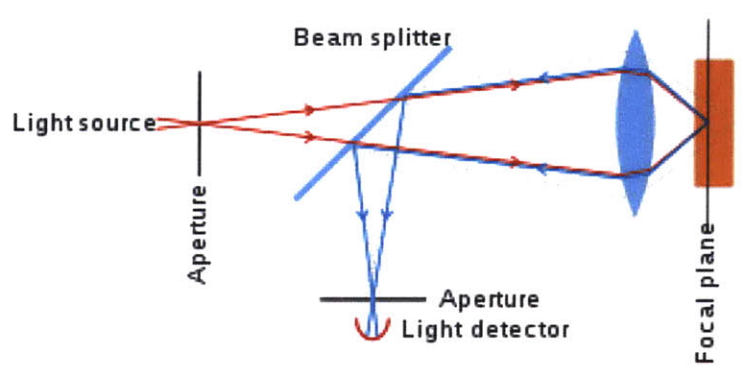


Figure 19: Principal of Con-Focal Microscopy ^[23]

Adjusting the position of lens could allow light detector capture the sharpest image of the targeted area. Most of current con-focal measurement systems are using CCD to detect the target and measure its position.

In this project we are using Nikon VERITAS VM250 as our main metrology to test the surface flatness through measuring the depth of the sample points. The following is the summary of general characteristics of Nikon VERITAS product series.

Size: Main body - 565 x 690 x 740 mm (minimum height), 72kg; Controller - 145 x 400 x 390 mm, 13kg

Cost: Depends on the type the precision and measurement range, more than \$10,000

Measurement Range (span): could achieve 50mm

Accuracy: could achieve 1 μm

Repeatability: rely on xyz moving stages

Resolution: Can achieve 0.1 μm

Power: AC100-240V \pm 10%, 50/60Hz

Environment Effect on Accuracy: within allowable operating environment, the accuracy can be well maintained

Allowable Operating Environment: Temperature - 10°C to 35°C; Humidity - 70% or less

3 Methodology

3.1 Stamp Casting Machine

Before processing the casting machine compatible with 12" master, we started with a 6" casting machine to see the capability of the design and building material (316 Stainless Steel). The design allows both 150mm wafer and 200mm wafer to be used in the same configuration. The stamp-casting machine will be capable of alignment for different masters. We use pins to locate wafer. In order to hold tight the wafer during pouring PDMS, grooves are designed for vacuum capability and wafer will be held using vacuum after aligning (see figure 20). Because no glue or tape will be used in the process, wafer will be easily replaced once the vacuum has been turned off.

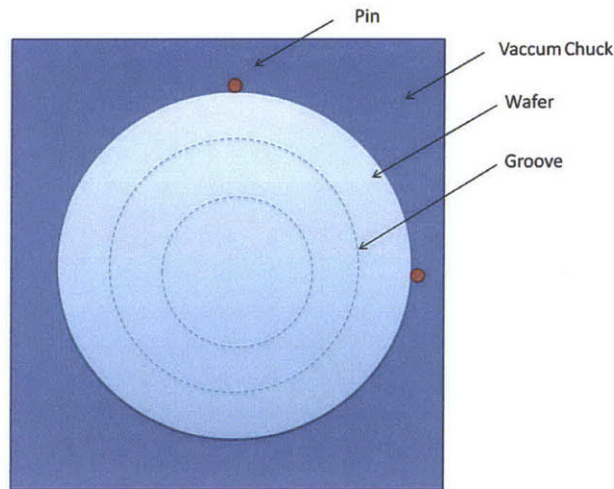


Figure 20: Structure for Wafer Chuck

A single piece of Teflon with a rectangular opening inside will attach to master as the dam for holding PDMS within the area, this Teflon will also act as spacer between master and backing plate (see figure 21). Shape and the thickness of the stamp on the backing plate are determined by this Teflon.

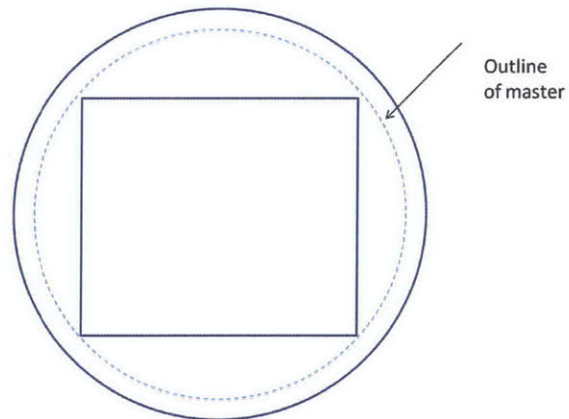


Figure 21: Teflon Spacer

The area for containing PDMS is confined by:

1. Wafer on the top for transferring pattern;
2. Thin stainless steel sheet (backing plate) sitting at the bottom as the backing for PDMS;
3. Dam between wafer and backing plate for holding the PDMS.

Repeatability is the critical design specification. Under this configuration, making a single big stamp will require many identical steps, and each step will result in a small area of finished stamp. Variables to be considered are:

1. Distance between master and backing plate (all attached to the chuck)
2. Displacement between master and backing plate
3. Uniformity of the stamp

All these variables can be decomposed in 6 dimensions: 3 linear and 3 rotational.

A sidebar is used to align both chucks, as shown in figure 22. The backing plate chuck (referred as SS Vacuum Chuck) is fixed to the side bar, while the adjunction of wafer chuck and sidebar leaves some clearance for adjusting. Minor adjustment is done by using screws to locate wafer chuck in both X and Y directions. The Z direction, also determines the height for stamp, is fixed by the thickness of dam.

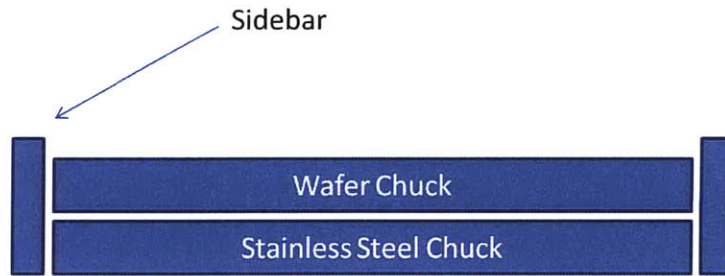


Figure 22: Sidebars Used to Align Both Chucks

Because the fabrication of stamp from PDMS is done in a low-pressure environment, the chucks with dam inside will be clamped together with strong force to ensure no air leaks in. Traditional C-clamp does not fit here because point contact will create distortion. Our approach needs to distribute the force as uniformly as possible. A clamping bar connected to sidebar by screw is used to provide clamping force. Small precision springs will be inserted between the clamping bar and wafer chuck to apply equal force.

3.2 Peeling and Wrapping the Stamp on the Print Roller

The R2R machine that was built by MIT'08 group proved that the R2R technique is feasible with micro-contact printing technology, but experiments showed that the printed images were affected by many distortions. The current way to wrap the PDMS stamp on the print roller is performed manually using a seam on the cylinder.

The challenges in the manual wrapping process using a seam demand the intervention of a skilled operator, making the process both time-consuming and labor-intensive. Also, even if all the operations will be performed in the correct way is not possible to guarantee the 5 microns alignment as required.

Therefore, the first goal of the project consists of improving the printing quality, designing a way to peel and wrap the stamp that will respect the following aspects:

- Maintain alignment
- Fast replacement

3.2.1 Gripping the Film for Peeling

The setup of the print roller before wrapping process is shown in figure 23. This setup comes after flat stamp fabrication process: disassembling the vacuum chuck from the fabrication device and placing the print roller at the edge of the backing plate.

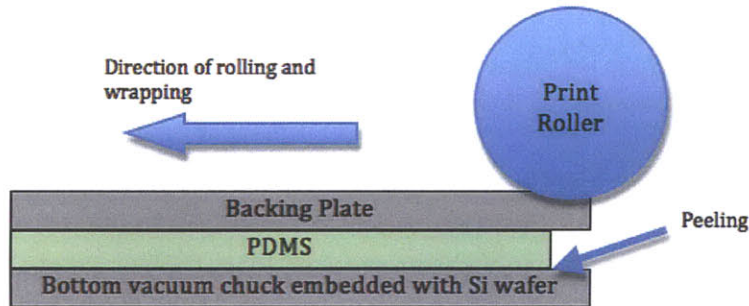


Figure 23: Illustration of Print Roller Setup Before Wrapping

Any device that grips the backing plate for peeling off the stamp must accomplish three steps in the peeling process:

1. Initiate the peel
2. Separate the film from the wafer
3. Transport the peeled film away

Unfortunately, the first and second stages are complicated by the inherent physics of peeling that we discussed in the literature review in the previous chapter. Let us begin by looking at the initiation of separation. This is a difficult step because the PDMS film adheres over the entire area of the substrate, leaving no 'lip' to hold the film or to start the separation. When an operator introduces a lip by inserting a razor, she must be careful not to scrape the film or inadvertently cut through it. Once she initiates separation, the operator may pull the film at point-contacts, which may cause excessive stresses and risk tearing around the contacts. If the film is adhered well to the substrate, she may need to pull hard on the PDMS film, which could also cause tearing.

Therefore, it is necessary to design a system that is able to grab and wrap at the same time the PDMS stamp that performs the following:

1. Grab the PDMS stamp without causing breaks or plastic deformations
2. Keep peeling the PDMS stamp applying a force with constant intensity, constant direction, and with a uniform distribution.
3. Wrap the PDMS stamp on the roller without losing alignment and without causing relative motion between cylinder and backing plate.

Keeping in mind the above requirements, we designed and analyzed concepts for peeling and wrapping the PDMS onto the backing plate. These concepts have been summarized below.

It should be noted that, based on the results of the MIT '08 project, it is evident that this step of peeling and wrapping with precision and alignment is the most crucial step, in that it has a direct bearing on the printing quality.

3.2.2 Methods to Generate Adhesive Force Between Backing Plate and Print Roller

Through the industrial investigation, we summarized the concepts, which is available on the market, to search for optimal solution the generate adhesive force between backing plate and the print roller:

1. Electro magnet cylinder.

It has ability to switch on and off the magnetic force of attraction, thus enabling better manual control over the pre-alignment of the print roller positioning with respect to backing plate.

However, the electro magnet cylinder requires additional electrical components and needs complex additions or modifications to print roller.

2. Permanent magnetic cylinder.

It could provide strong magnetic force, even if rare earth magnets used, which is easily available.

On the other hand, permanent magnetic cannot switch off magnetic force. Also to machine a cylinder with permanent magnetic force is expensive and difficult to obtain precision in diameter and tight tolerances.

3. Cylinder with vacuum force

The vacuum holes along the cylinder could provide uniformly distributed attraction force along surface of cylinder. The vacuum cylinder is adaptable from existing commercial vacuum rolls.

Nevertheless, the vacuum cylinder requires additional vacuum pump and vacuum control. And backing plate will have to cover entire vacuum-surface of cylinder; otherwise leakage of vacuum could be an issue.

4. Cylinder with double sided adhesive tape on the surface

Attaching the double-sided tape onto the surface of the cylinder could also provide strong adhesive force and such design is obviously simple and easy.

The disadvantage of this method is that the double-side tape Introduce another layer between the print roller and the backing plate which another source of variation on the roundness of the roller. In addition, it is difficult to correct errors of misalignment of backing plate with cylinder. Furthermore, cleaning cylinder for stamp replacement would be very difficult.

Chosen Method: Through analyzing above those possible solutions of the print roller, we finally decided to use stainless steel cylinder with a series of permanent magnets embedded into the cylinder.

This kind of cylinder is a well-established design for use in the die-cutting and embossing industry, hence easily available.

Also, this design satisfies all the precision and accuracy requirements with respect to the diameter, total run out, and straightness of the cylinder.

3.2.3 Methods to Wrap Backing Plate without Loosing Alignment

1. Slot in print roller, clamp to grab backing plate

Clamp refers to an L shaped projection that would slip between the backing plate and the Si wafer. This would enable a positive grabbing or locking of the backing plate with the print roller, it requires pre-alignment before clamping.

2. Slot in print roller, bent edge of backing plate

This would be similar to using a clamp, except that the backing plate would be bent, and would stick out, enabling one to insert the bent edge into a slot in the print roller, again accomplishing a positive locking arrangement. But the relative position of the edge of backing plate and the slot has to be very accurate in order to maintain the alignment.

4. Pins in roller, holes in backing plate

This design consists of two (or more) pins inserted using threaded holes in the body of the cylinder. Corresponding holes would be drilled or machined in the backing plate. The height of the pins sticking out of the cylinder would be less than the thickness of the PDMS (less than 500 microns). This would prevent damage to the wafer during peeling and to the substrate during printing. Also the pins and holes could provide enough assembly constraints to guarantee desired alignment.

Chosen Method: Pins in roller, and holes in backing plate. This was found to be the simplest, easiest to adapt, and the most precise design.

3.2.4 Analysis of Fixture System

A fixture system that helps to guide the movement of the print roller during the wrapping was designed, as shown in figure 24.

The fixture would serve two purposes:

1. Pre align cylinder with backing plate
2. Maintain alignment during wrapping of the backing plate on the cylinder

However, the fixture system over constrains the cylinder-backing plate during wrapping. This is because, the force of adhesion between the cylinder and backing plate already achieves alignment

between the two. Hence, if the fixtures try to achieve a slightly different alignment, it would create distortions and twisting forces in the backing plate, which would lead to detrimental effects on the stamp, and induce unwanted stresses in the stamp.

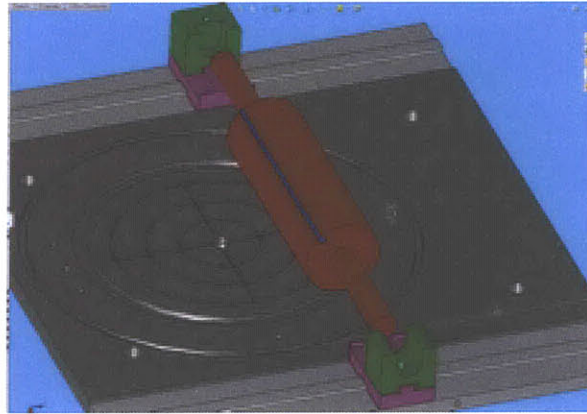


Figure 24: Illustration of the Proposed Fixture System

Upon conducting experiments with a prototype Aluminum cylinder, with pins, and holes on backing plate, and conducting error analysis for the same, it was decided that pin-holes are the best way to minimize alignment errors between the backing plate and print roller. Thus, the fixture system was not used.

3.3 Precision Measurement Method

The initial purposes of this project were to fabricate a stamp with uniform thickness, wrap the stamp onto the roller with uniform roundness and to demonstrate multi-layer printing. In order to answer the questions such as how thick the stamp is, how flat the stamp is, how good the quality of multi-layer printing is and etc., a thorough measurement method need to be develop to precisely and correctly answer those questions. Meanwhile, multi-layer printing requires upgrading the accuracy of alignment of the current R2R system, so a systematical measurement is also desired to demonstrate the improvement of alignment in accuracy.

3.3.1 Flatness and Roundness Measurement

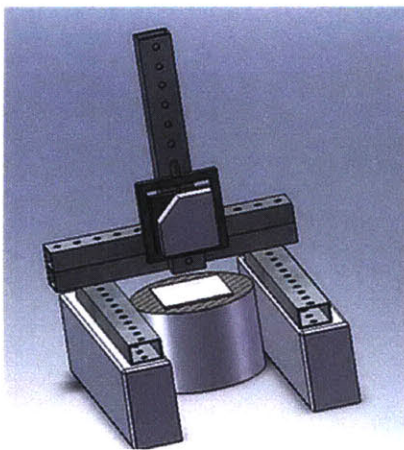
In the stamp fabrication and wrapping process, the ultimate goal is to make sure that the diameter of print roller has the variance of $\pm 4\mu\text{m}$, and the print roller here means the assembly of the central shaft, sleeve, and the backing plate with the stamp. All the potential variance could be broken down into following categories:

- Flatness measurement
 - Flatness of stainless steel
 - Flatness of the PDMS stamp
 - Uniform thickness of attached PDMS on stainless steel
 - Flatness of devices that used to fabricate the stamp
- Roundness measurement
 - Roundness of print roller
 - Roundness of central shaft
 - Eccentricity of the motion of the driver motor

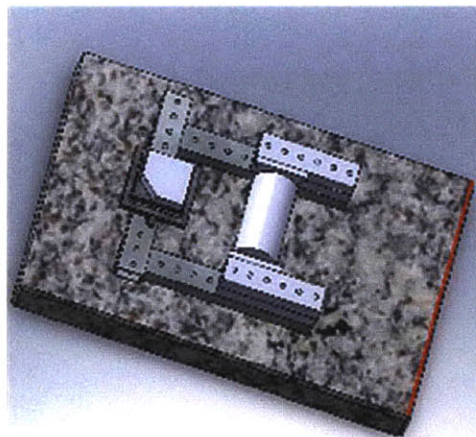
Due to the specific characteristic of PDMS and the overall process, the measurement device should obtain following requirements:

- Non-contact measurement
- High resolution, targeting on $1\mu\text{m}$
- Sufficient measurement range ($>1\text{mm}$)
- Affordable

At first, Laser triangulation sensor was the first choice, which is perfect aligned with all above requirements. Corresponding fixtures and frames were developed for the flatness and roundness testing, as illustrated in Figure 25. Basically, the laser sensor sits on the micrometer head for the fine adjustment and the micrometer head is mounted onto the frame to test either flat or round surface.



Flatness measurement



Roundness measurement

Figure 25: Fixtures for Flatness and Roundness Measurement

However, the chosen laser sensor cost more than \$4000 and could only be used for this project in the view of Nano Terra LLC, which is not cost effective for the company in sake of the future application. Therefore, we plan to use the available CNC Video Measuring Systems (Nikon VERITAS VM 250) that could measure the height of the surface by using con-focal technology. (The machine is shown in figure 26)

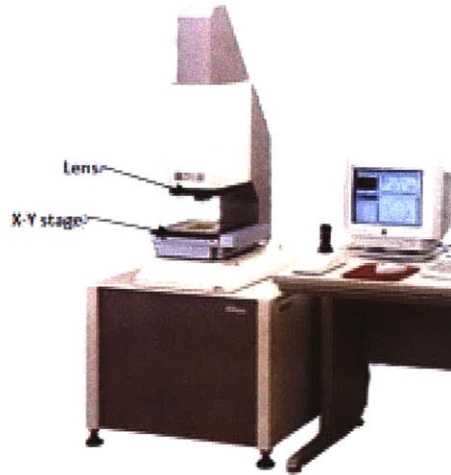


Figure 26: VERITAS VM 250

To measure the flatness using Veritas, the object should be placed onto the x-y stage and measure the height of sample points on the surface of the object. Since the x-y stage could move along x and y axis in a perfect flat surface, it help to keep away from the disturbance introduced by the measurement equipment.

Roundness of the print roller is targeted because of its critical impact towards the printing quality. Although the roundness of print roller is very forgiving in self-assembly materials and the impression roller, which contacts the print roller during the printing process, could tolerate the variance of the roundness, the high roundness print roller is still desired in the view of future development. Because, if using some other materials that do not have self-assembly characteristics or very little pressure could be applied onto the print roller, a perfect roundness print roller is highly important to the final print quality.

In actual measurement, there is a problem with the roundness test due to the optical property of PDMS. PDMS is elastic transparent material that does not allow the laser sensor or the dial indicator to precisely measure the roundness variance. A few solutions could be applied to solve this issue: An Interferometer is not limited by such kind of materials but it is too expensive for this project, or the stamp could be coated with metal powder and then use laser sensor to measure the distance, but this method will cause the damage of the stamp. Finally, the roundness of the printer roller could be indirectly indicated by the accumulate effect of the roundness of the print

roller with the stainless steel sheet and the flatness of the stamp. The stamp is seamless attached to the stainless steel sheet; therefore, we assume the variance caused by the attachment is zero.

In the roundness test, since we are only interested in how round the print roller is when it is rolling for printing and we are trying to compare the different performance of two wrapping systems, the measurement is taken separately into two systems (i.e. previous R2R system and updated R2R system) while simulating a real printing process. The final roundness information of the print roller is the aggregated result of the motor shaft eccentricity, motion transition quality of the connected bearings, roundness of the central shaft, roundness of the sleeve, variance caused by assembling the sleeve on the shaft, firmness of the attachment between the stainless steel sheet and the sleeve, and the flatness of the stamp. A dial indicator was used to make this measurement and figure 27 illustrates the general idea of the measurement settings.

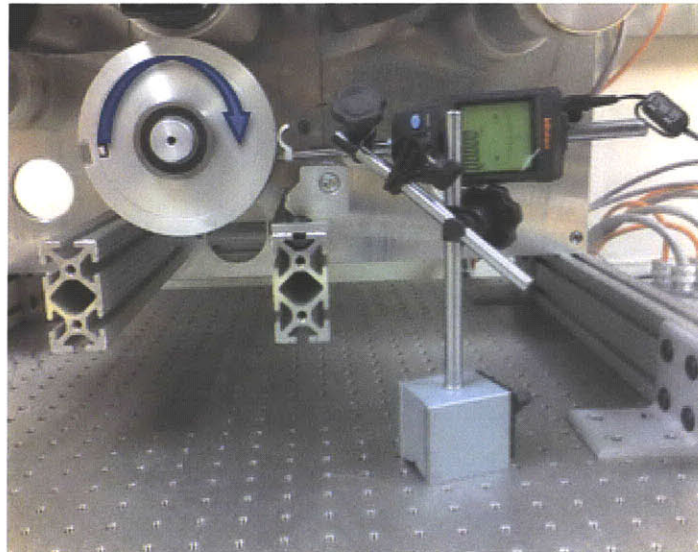


Figure 27: Measurement Setting for Roundness Measurement

With each rotation of the print roller, 16 sample points were collected at 3 positions along the roller (Front, Middle and Back) are test, which means 16x3 sample points are collected for roundness analysis.

3.3.2 Distortion Measurement

After the features are successfully transferred from the stamp to the substrate (gold coated PET is the substrate used in this project), one of the most important quality indicators is the distortion of pixel on the substrate. The distortion is caused by several reasons:

1. Distortion of the flat stamp during the fabrication process
2. Distortion caused by wrapping the stamp onto the print roller
3. Tension in the substrate during printing

4. Deformation of the stamp from print pressure

All above sources of the distortion had been carefully analyzed in the thesis of *Analysis of the Capabilities of Continuous High-Speed Micro-contact Printing*^[20] by Kanika Khanna. Based on her study, the wrapping process contributes the most to the final distortion.

The overall pattern printed comprises two types of pixel patterns, rectangular and triangular, as shown in Figs 28 and 29. The array of both of these pixel patterns is shown in figure 30, where each pattern is printed on a 1.5mmx1.5mm square^[20].



Figure 28: The Shape of Rectangular- like Pixel

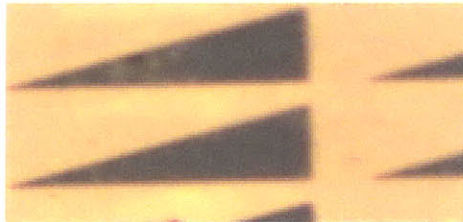


Figure 29: The Shape of Triangular Pixel

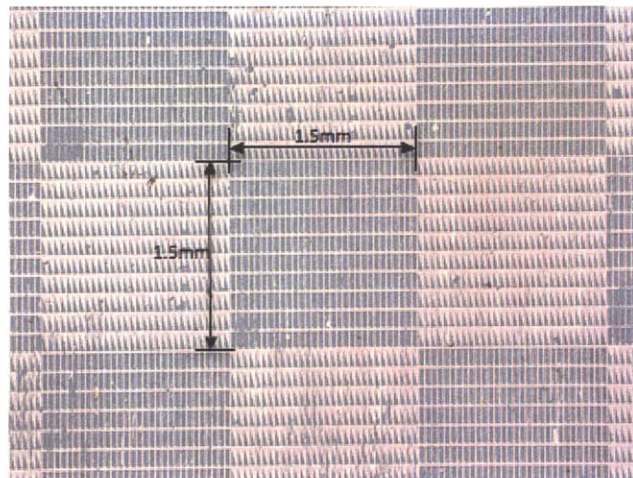


Figure 30: The Array of Two Kinds of Pixels

As mentioned before, the wrapping process causes distortion of the stainless steel sheet, which is used to hold the stamp in the printing process. The distortion of the stainless steel sheet leads to distortion of stamp, and hence the distortion of pixels. Figure 31 demonstrates the distortion of pixel in a simply way. The black dashed rectangle is the standard shape of the pixel on the substrate and the blue solid rectangle is the distorted printed pixel. In figure 31, X and Y indicate the horizontal and vertical dimension of the standard pixel; X' and Y' indicate the corresponding dimension of printed pixel. It is important to note that the shape of distortion varies based on multiple reasons. To indicate the distortion, we will just simply use Y'/Y and X'/X as the distortion rate to identify the distortion over the Y and X axis

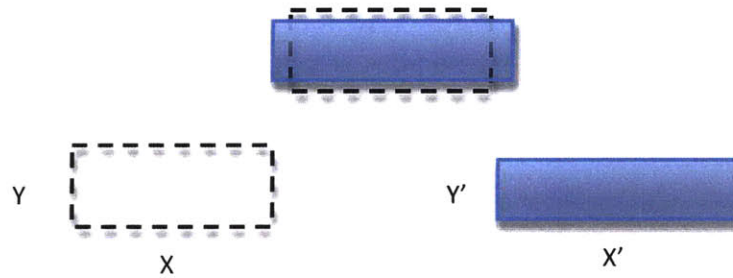


Figure 31: Demonstration of the Distortion

In order to make things easy, the distortion measurement is only taken on the rectangular-like pixels shown in figure 28, which is statistically representative to the overall distortion. For those rectangular-like pixels, their standard dimension is $130\mu\text{m} \times 40\mu\text{m}$ as shown in figure 32.

It is important to distinguish pixel distortion from pattern distortion. In this work we concentrate on distortions of at the pixel level, and are not concerned with overall pattern distortion caused by web movement or a non-parallel stamp on the roll. The stamp is made from a 300mm wafer, and the actual size of the square stamp is 200mmx200mm. This area is evenly divided into 5x5 cells with each cell being 40mmx40mm. Within each cell, 5 pixels are randomly picked to measure, and averages to minimize the measurement error. This average is used to represent the dimension of the pixels in this area.

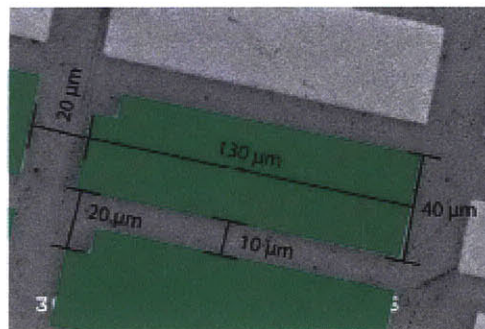


Figure 32: Pixel Dimensions ^[20]

3.3.3 Measurement of the Accuracy of the Alignment

The scope of the multi-layer printing in this project is to use the stamp print twice on the same substrate without losing alignment. Therefore the accuracy of the alignment could be measured by indicating how well the overlap of two printed features, shown in figure 33. In current stage, only x and y displacement are concerned. The angular misalignment is not included in the measurement due to the time constrain.

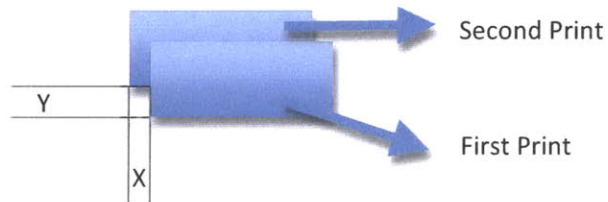


Figure 33: Displacement of Two Printed Layers

Same to the measurement of distortion, 5x5 matrix divided the 200mmx200mm printed area into 25 squares. Take the average of 4 measurement within each square for the x and y displacement.

4 Final Design: Results and Discussion

In this chapter, the final design of four key components is described. The reliability, repeatability and accuracy of the updated R2R printing system is assessed by measuring the quality of the critical components, distortion of the single layer printing and the accuracy of alignment of the multi-layer printing. The means of the measurement has been reviewed in the Chapter 3, and in this case, laser sensor, electronic microscope, optical measuring system and dial indicator are adopted to serve different measurement purposes that will be explained in following paragraphs in details.

In this chapter, four key components of this project are introduced and measured: flat stamp fabrication, wrapping process, single layer printing with updated R2R machine and multi-layer printing. Within each component, the updated design of process, comparison between updated system and previous system and measurement results will be carefully reviewed.

4.1 Flat Stamp Fabrication

4.1.1 Updated Flat Stamp Fabrication Device

This section is an excerpt from Yufei Zhu's thesis ^[29]. The section below briefly describes the updated flat stamp fabrication device. For more details, please referred Yufei Zhu's thesis ^[24].

The new stamp fabrication device is a mature version of the old device mentioned in chapter 3. 1. Improvements of this new design include:

1. The pattern can be changed easily and quickly aligned
2. Flatness of stamp is at the level of microns
3. The backing plate is mechanically aligned during stamp fabrication
4. Both chucks used in this device can be disassembled to remove PDMS
5. The machine is capable of maintaining low pressure in internal area during stamp pouring

4.1.1.1 Wafer Chuck

A Wafer chuck is used to hold the wafer with a vacuum and 3 wafer chucks have been designed to apply for different size of wafers, including 6", 8" and 12" diameter silicon wafer. The design of wafer chuck (shown in figure 34) has concentric grooves. A wide circular tunnel has been added outside the grooves to prevent PDMS from leaking into vacuum area below the wafer. Pins are used to locate wafer before vacuum is applied. A Hose will be connected to the wafer chuck for PDMS injection.

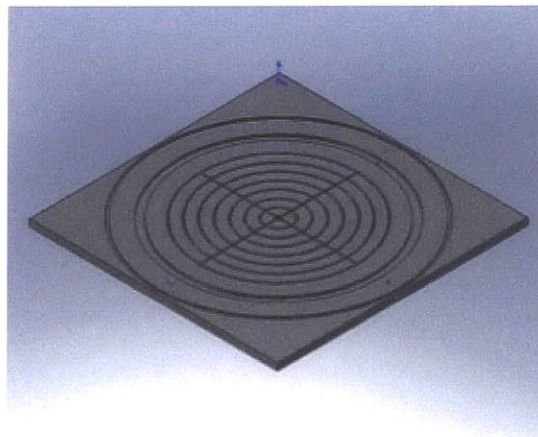


Figure 34: 3D Model of Wafer Chuck for 12" wafer

4.1.1.2 Stainless Steel Vacuum Chucks

Stainless Steel (SS) Chucks are used to hold the backing plate (SS Sheet) onto which PDMS will adhere. The SS chuck is intentionally divided into several parts and assembled together, allowing holes and vacuum channels to be cleaned whenever they are jammed by PDMS. In addition, the parts of the vacuum chuck can be assembled in different ways to match different wafer chucks. Figure 35 shows the 3D model of SS vacuum chuck for 200mmx200m stamp fabrication. The upper part in the picture is the adapter complying with 12" wafer chuck with which the largest area stamp (200mm X 200mm) is produced. This adapter has tunnels below the holes that are complementary to holes in the top SS chuck.

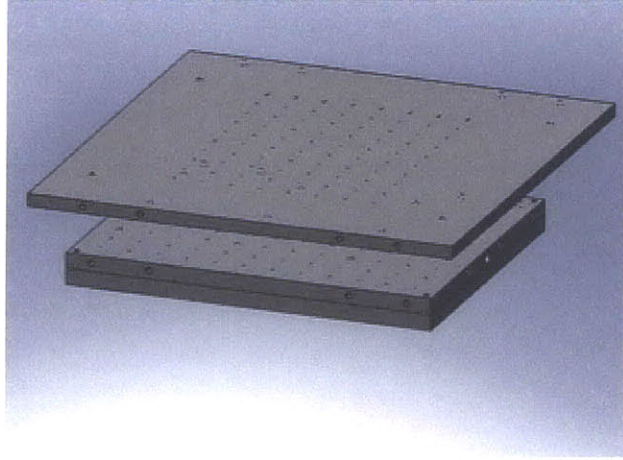


Figure 35: 3D Model of Adapter of SS Chuck for 200mmx200mm Stamp Fabrication.

4.1.1.3 Assembly of Stamp Fabrication Device

Assembly of the stamp fabrication device follows the method mentioned in Chapter 3.1. And the 3D model of the assembled device is shown in figure 36. The wafer chuck is represented by a wireframe for clear view inside the structure. Two other clamping bars will be added during stamp fabrication. The location of clamping bar is determined by the location of threaded-holes at the sidebar.

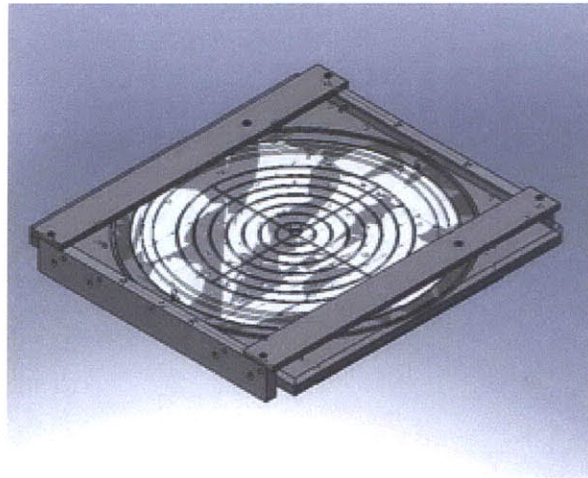


Figure 36: 3D Model of Assembly for 12" wafer.

4.1.2 Measurement of Flat Stamp Fabrication

This section focuses on the measurement of the flatness of vacuum chuck surface, flatness of the stamp surface and the thickness of the stamp.

4.1.2.1 Measurement of the Flatness of Vacuum Chuck Surface

As mentioned above, in order to fabricate the flat stamp with the variance of $4\mu\text{m}$, the parts involved in fabricating the stamp must have perfectly flat surfaces. These parts include the stainless steel sheet, vacuum chuck, wafer chuck and the wafer. Among all the parts, the vacuum chuck used to hold the stainless steel sheet is the most critical one because the other parts that related to the stamp flatness including wafer and stainless steel sheet, are standard parts that are typically very flat. As for the wafer chuck, since it is used to hold the wafer, the flatness of the wafer determines the flatness of the stamp.

The vacuum chuck was made of aluminum in 2008, which limited the surface hardness and hence affected the durability of the flat surface. This year, the vacuum chuck is made of stainless steel sheet with precision grinding. The physical appearance of the backing plate vacuum chucks is shown in figure 37 and 38.

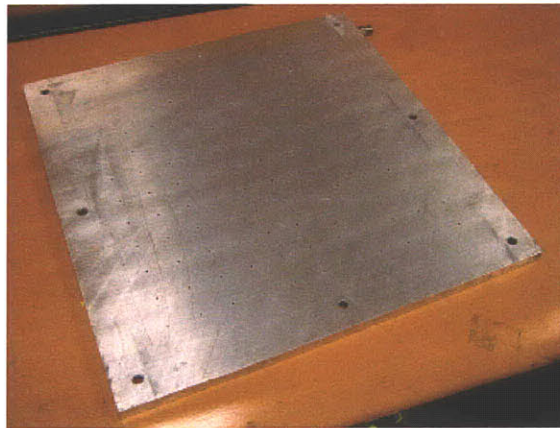


Figure 37: Aluminum Vacuum Chuck Used in Last Year's Project

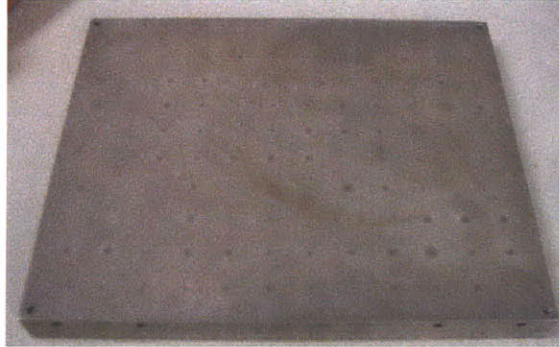


Figure 38: Stainless Steel Vacuum Chuck Designed and Machined This Year

To measure the surface flatness of vacuum chuck, a Nikon VERITAS 250 was used to measure the height of surface using con-focal technology. By placing the vacuum chuck on the platform of the VERITAS, the central 10x10 points are measured within the range of VERITAS device, which is shown in figure 39.

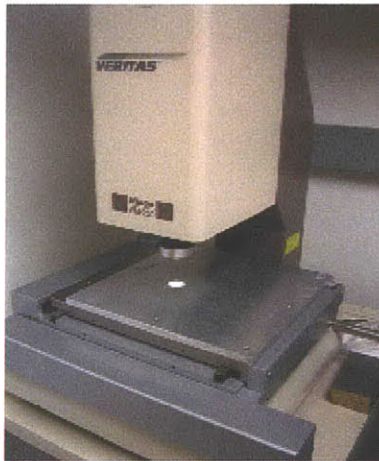


Figure 39: Using VERITAS 250 to measure the flatness of the vacuum chuck

After getting the height 10x10 points of two vacuum chucks, the data has to be adjusted by eliminating the slope impact of the measurement platform. With two sets of 10x10 points, the topographic charts of two vacuum chucks are plotted and shown in figure 40 and figure 41. In these two charts, the base coordinate shows the X and Y position of 10x10 points and Z axis denotes the height of corresponding point.

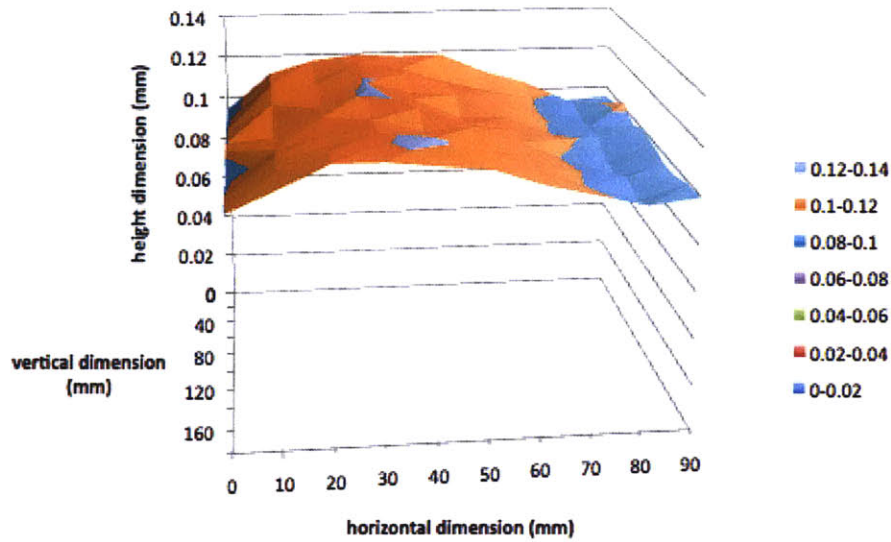


Figure 40: Topographic Mapping of the Previous Vacuum Chuck

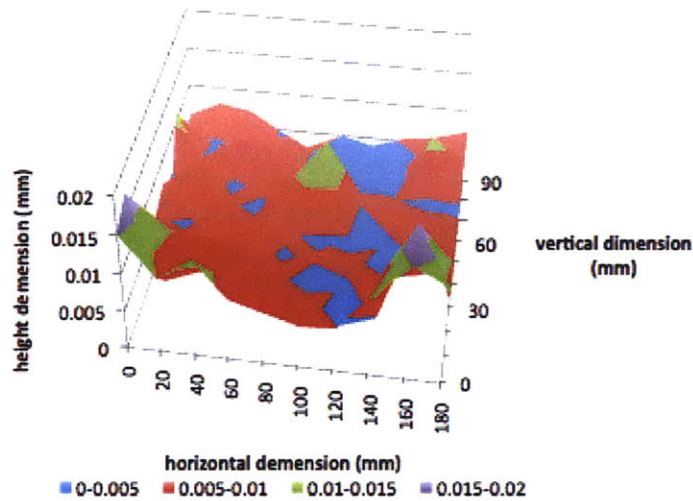


Figure 41: Topographic Mapping of New Vacuum Chuck

After taking QQplot test on both test results, as shown in figure 42 and 43, we found that the data for the previous vacuum chuck is not normally distributed owing to the obvious bow shown in Fig. 40 but the data for the new vacuum could be considered as normal distribution. A Histogram for the new vacuum chuck test result is shown in figure 44. Based on the topographic mapping as well as the data analysis, we found that the range of the flatness of previous vacuum chuck is $32\mu\text{m}$, comparing to $22\mu\text{m}$ of the flatness of this year's vacuum chuck. Also the standard deviation of the flatness for the new vacuum chuck is $3.6\mu\text{m}$.

Another serious problem of last year's vacuum chuck is that there is bow curve (shown as orange color in figure 40) on the surface that would cause slight bending of the SS sheet and hence impact the quality of the stamp fabrication. This pattern could also explain why the test result for the previous vacuum chuck does not follow standard distribution.

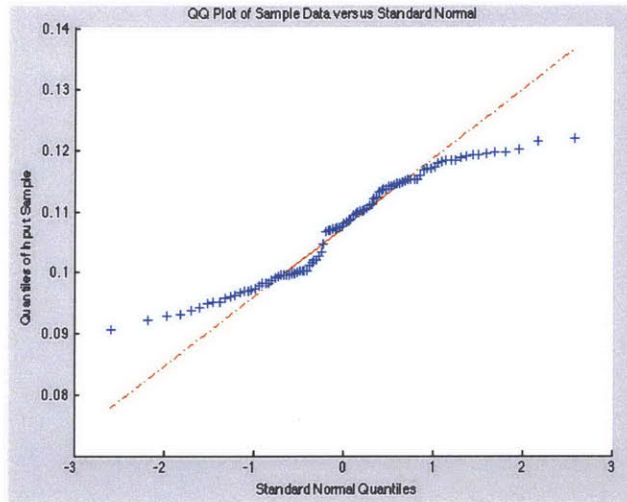


Figure 42: QQplot of The Test Result of The Previous Vacuum Chuck

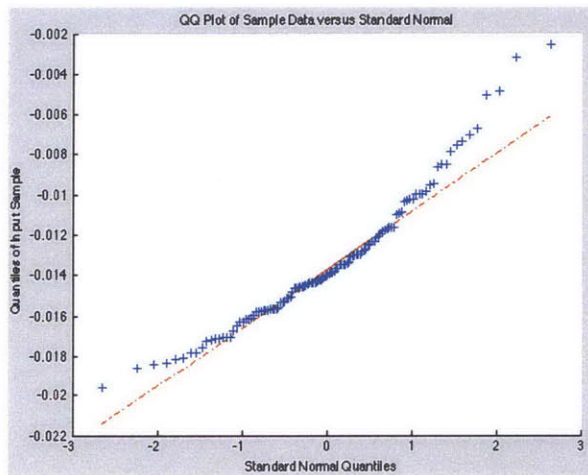


Figure 43: QQplot of The Test Result of The new Vacuum Chuck

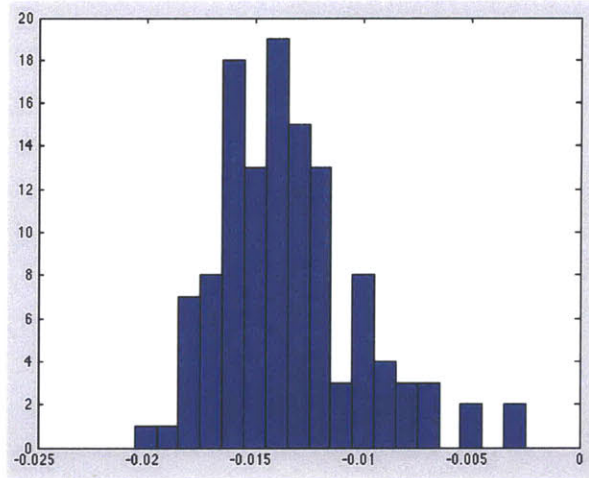


Figure 44: Histogram of The New Vacuum Chuck Test Result

4.1.2.2 Measurement of Flatness of The Stamp Surface

By using two different flat stamp fabrication devices, two stamps are prepared. Both stamps are stuck to the stainless steel sheet, and the stainless steel sheet is held by a vacuum chuck. The flatness of the stamp is tested by measuring the height of the stamp that supported by stainless steel sheet sitting on the vacuum chuck.

Since the SS sheet always goes with the stamp through out the printing process, it is reasonable to measure the flatness of the stamp together with the SS sheet. However, holding the SS sheet with the vacuum chuck is not an optimal solution in this measurement, because the flatness variance of the vacuum chuck's surface would impact the result. Even though, vacuum chuck is the only solution so far that can be used to hold the SS sheet firmly on a comparatively flat surface. Actually, with such setup, we measure the flatness of the stamp first and then remove the stamp with SS sheet to measure the same area of the vacuum chuck (the result is shown in section 4.1.2.1), trying to minimize the interference.

As with the vacuum chuck, 10x10 points of the stamp are measured; the data has to be adjusted by eliminating the slope impact of the measurement platform. With two sets of 10x10 points, the topographic mappings of two stamps are plotted and shown in figure 45 and 46.

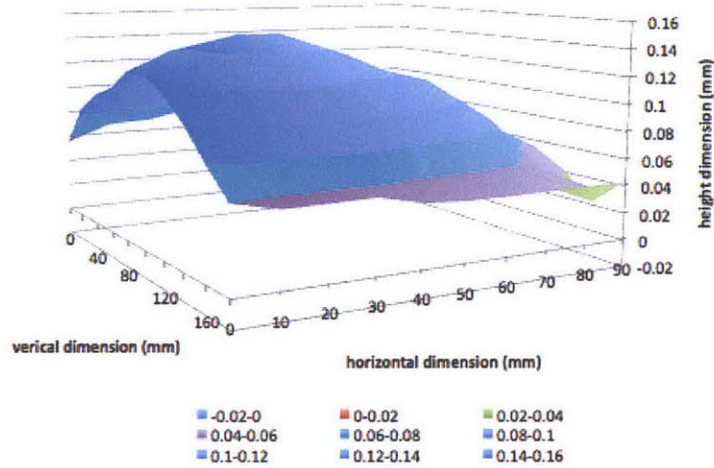


Figure 45: Topographic Mapping of The Stamp Fabricated Using Last Year's Device

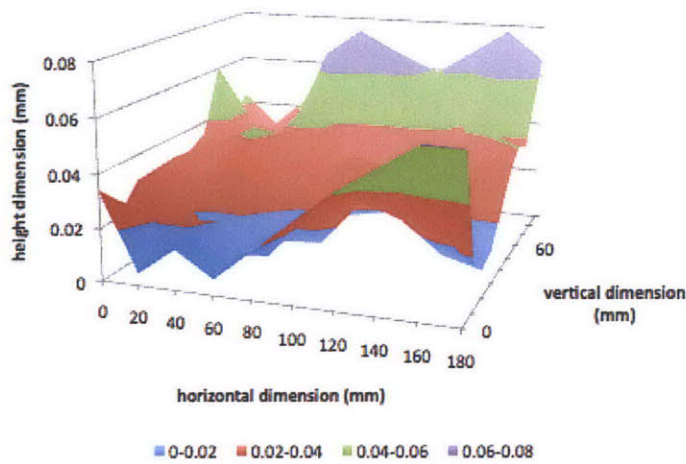


Figure 46: Topographic Mapping of The Stamp Fabricated Using New Device

After a QQplot test on the test result for the stamp fabricated with new stamp, as shown in figure 47, we could tentatively treat the distribution as normal distribution. As for the test result of the stamp fabricated by last year's device, its topographic mapping already suggests that the data is not normally distributed. The standard deviation of the flatness of the stamp with new device is $16\mu\text{m}$.

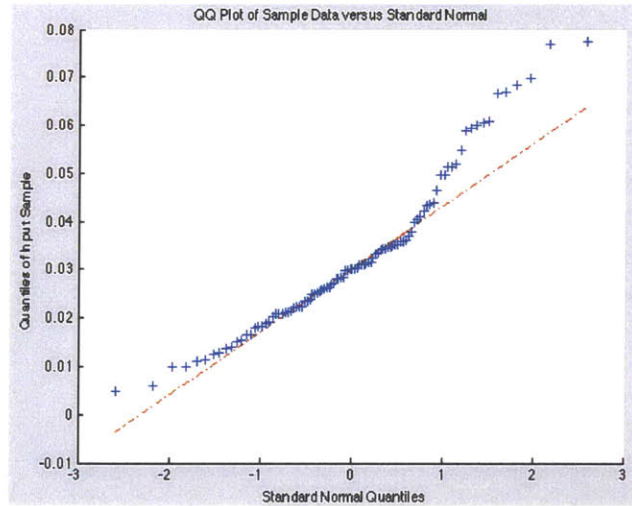


Figure 47: QQPlot of The Test Result for The Stamp Fabricated Using New Device

According to the topographic mapping, the curvature pattern of the stamp surface aligns with that of the vacuum chuck, which proves that the surface of the vacuum chuck does impact that of the stamp. After eliminating the impact of the vacuum chuck by deducting the data of vacuum chuck from the stamp surface measurement, the previous stamp fabrication process generates $125\mu\text{m}$ as the range of stamp's flatness, and the updated process has a range of $67\mu\text{m}$. Although the number about the variance of the stamp is not 100% accurate because of the stainless steel sheet property and deformation of the stainless steel sheet caused by the suction of vacuum chuck, a big improvement of the flatness of the stamp was observed.

4.1.2.3 Measurement of the Thickness of the Stamp

The flat stamp will be wrapped on the print roller, and we need to minimize the stamp distortion introduced during this process. Based on some simple calculations, it is easy to tell that when wrapping the stamp onto the roller, the thinner the stamp the smaller the perimeter's difference of the upside and underside of the stamp, and such perimeter difference is the source of the stamp distortion. Therefore, we were targeting on casing very a thin stamp with the thickness of $800\mu\text{m}$. The measurement of the stamp thickness was also done with the Nikon VERITAS. In this measurement, the stamp is peeled off from the stainless steel sheet and attached onto the cleaned platform with its adhesive back. As the measurement in the flatness, the height of the stamp is measured, as well as that of the surface of the platform.

After taking 40 sample points on the surface of the stamp and 10 sample points on the surface of the platform, we first adjusted the slope impact from the measurement platform and then calculated the thickness of the stamp by taking the height difference of the stamp and the platform. Using previous fabrication method, the average of the thickness is $875\mu\text{m}$ with $27\mu\text{m}$ standard

deviation. The updated method has the average thickness of $1194\mu\text{m}$ with standard deviation of $9\mu\text{m}$.

Admittedly, we did not reduce the thickness of the stamp, but the standard deviation of the thickness that could be considered as the flatness of the stamp is significantly improved. Since the thickness of the stamp is determined by the thickness of Teflon dam, a thinner stamp could be easily achieved as soon as the thickness of Teflon reduced. In our project, the vendor, who machined the Teflon dam, mistakenly used the 1.4mm-thick Teflon, which is not the appointed thickness of the Teflon. Due to the time constraint, we did not re-machine the Teflon dam, but we have confidence that a thinner stamp is easy to achieve.

4.2 Wrapping Flat Stamp onto The Print Roller

4.2.1 Updated Wrapping System

For the updated wrapping system, two major processes should be mentioned: alignment process and peeling process. Their functional requirements are:

1. Align SS sheet with the sleeve of the print roller
2. Peel PDMS stamp off the Silicon wafer
3. Wrap the PDMS stamp with the stainless steel backing plate onto the print roller
4. Maintain alignment of the stamp with the print roller during steps 1 and 2
5. Enable compatibility with the adjustment system

In the alignment process, the initial alignment of the roller with the backing plate would essentially define the precision of the rolling, and the quality of the print output. Thus, this alignment is critical. We chose a pin-hole and pin-slot combination as the means of this alignment, i.e. the print roller will have two pins that will mate with a hole and a slot respectively in the backing plate. The initial pre-peeling setup is shown in figure 25 at the methodology chapter. Once this alignment is established, the next step is to peel the backing plate attached to the PDMS stamp, while maintaining this alignment, and wrap the backing plate onto the print roller.

The magnetic cylinder must have the capability to peel off the backing plate with PDMS from the Si wafer while maintaining the alignment in continuous movement. Since the alignment of the backing plate with the magnetic cylinder must be achieved during the peeling process, the first contact between the magnetic sleeve and the backing plate must first define the alignment. Also with the precise alignment and the magnetic force around the sleeve which provides uniform adhesive force to attach the SS sheet, the distortion of pixels on the stamp is minimum and expectable. For detail information about the wrapping process design and development, please refer to Charudatta Datar's thesis "Design and Development of High Precision Elastomeric -Stamp Wrapping System for Roll-to-Roll Multi-Layer Microcontact Printing"

4.2.2 Measurement of Wrapping Quality

After wrapping the SS sheet with the stamp onto the sleeve and mounting the sleeve to the shaft, we want to know the straightness and roundness of the print roller when it is rolling. Due to the limitation of metrology system, the straightness of the print roller could not be measured in this project. However, the straightness is not a big concern in the printing process because the print roller is sitting on flexures, which could adjust the straightness with high repeatability and accuracy.

By analyzing two sets of 3x16 data points as mentioned in methodology chapter, we get the range of the roundness for the previous wrapping system is 1.36mm whereas the updated wrapping system has a range of 20 μ m.

Another big portion of the measurement of the wrapping process, although hard to quantify in this project, is the deformation of the stainless steel while wrapping. In previous wrapping system, two ends of the SS sheet have to be manually put into the slots of the stamp retainer bar and then screw the retainer bar into the slot of the sleeve, as shown in figure 48.

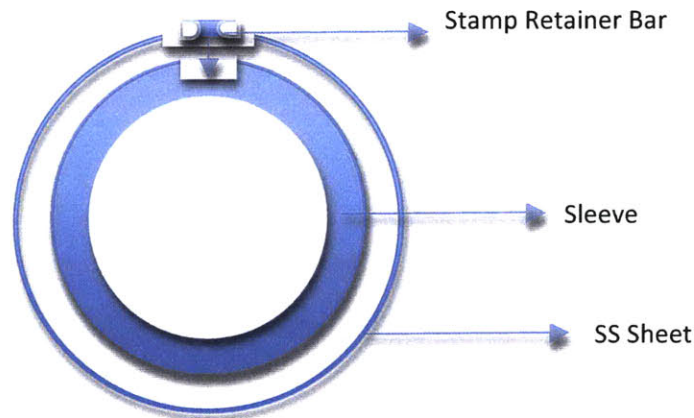
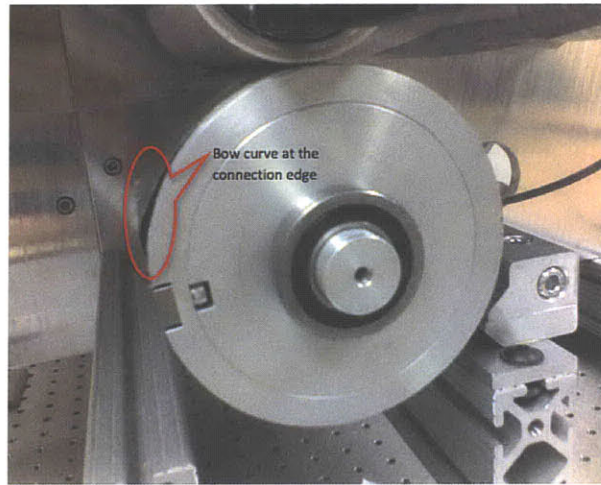
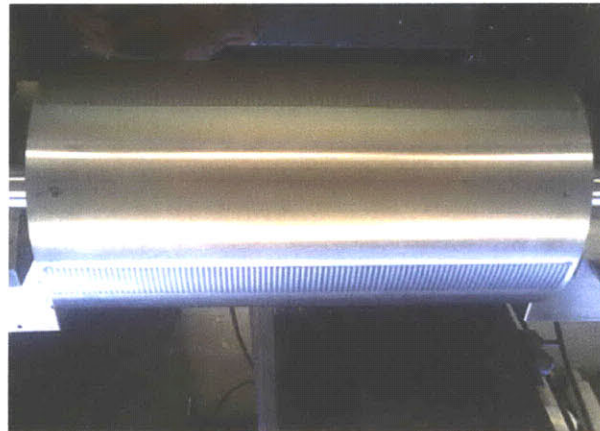


Figure 48: The Assemble Sequence of the SS Sheet

It usually takes 5 to 10 minutes to put the both ends of the 5-mil stainless steel sheet into the 2mm slot. In this process, the SS sheet may spring back several times. The biggest problem in this process is that it is almost impossible to guarantee that both ends of SS sheet are parallel in the slot; therefore, screwing the retainer bar into the sleeve will cause uneven distortion over the stainless steel sheet. Or some part of the stainless steel sheet may tightly attach to the sleeve, while other part is loosely attached. Such a situation would lead to a bow curve at the connection area of SS sheet and retainer bar (see figure 49(a)). While the upgraded print roller shown in figure 49(b) has magnetic strips that provide uniform attachment force over the backing plate, so the backing plate was sticking to the roller evenly and firmly.



(a)



(b)

Figure 49: Different Print Roller used in 2008 (a) and 2009 (b)

The Bow curve mentioned here could also be demonstrate with the sample points in the roundness measurement. In the chart below (see figure 50), three spikes show from point 3 to point 7, which are the connection area along 3 sample positions.

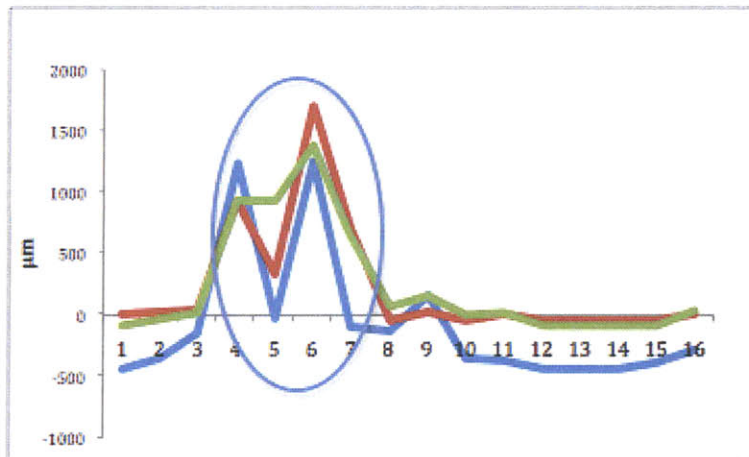


Figure 50: Roundness Test Result of Previous Wrapping Method

4.3 Single Layer Printing with Updated R2R Machine

4.3.1 Introduction of the Updated R2R Machine

The upgrade of previous R2R machine involves two major sub-systems : the print roller system and the impression roller system. The upgrade of these two systems allows the machine to adjust the relative position of the print roller and the impression roller to within of $1\ \mu\text{m}$, significantly improve the repeatability of the movement of both sub-systems and reduce the external disturbance over the printing process.

4.3.1.1 Upgrade of the Print Roller System

This section is the excerpt from Paolo Baldesi's thesis "Design and Manufacturing of High Precision Five Axis Positioning system for Roll-to-Roll Micron Contact Printing" ^[26]. Please refer to his thesis for more detail information.

The final design of the print roller system involves the use of two flexures, five micrometer heads, five fixtures for micrometers heads and a flexible coupling. Flexures are monolithic blocks, they allow very smooth movements relying on the elastic properties of the material of which they are made. Furthermore, the monolithic piece does not introduce new variability in the system and, using micrometer heads, is possible to smoothly and accurately drive the flexure motion. Both flexures have the same structure shown in figure 51. The selected micrometers have a resolution between $1\ \mu\text{m}$ and $2.5\ \mu\text{m}$ and accuracy between $0.5\ \mu\text{m}$ and $1.5\ \mu\text{m}$.

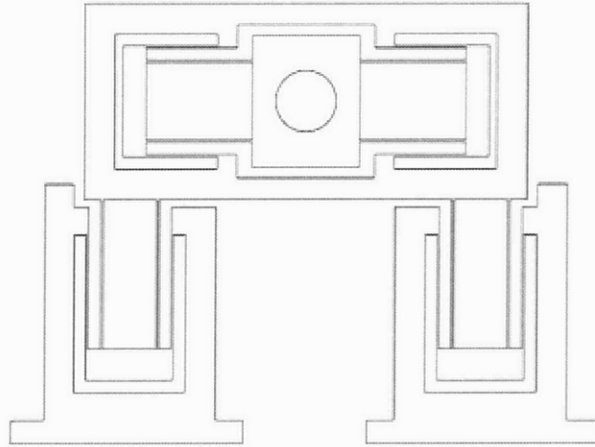


Figure 51: Structure of the Flexure (Front View)^[26]

The design is composed of following components: front flexure, back flexure, horizontal fixtures, vertical fixtures, and frontal flexure. Each component is mounted on an optical table to ensure alignment of all components within the adjustment system and with other modules of the machine.

The shaft on which is mounted the magnetic sleeve, is inserted in the flexures through two linear/rotary bearings, which allow the shaft in rotating and sliding along the Y-axis. The bearings are press fit in the center of the flexure. Finally the shaft is attached to the motor using flexible couplings that allow a lateral, angular and axial displacement.

The Print Roller is supported by the flexures and it is connected to the motor through a flexible coupling. The micrometer heads are supported by the fixtures and in contact with the flexures. Micrometer heads are fixed on the fixtures with a clump nut and they are responsible for the fine adjustments. After the adjustment, the micrometer will be locked and the flexure, constrained by the micrometer, will stay in the new position. Therefore the print roller can rotate with the flexure-micrometer system behaves as a rigid system. Vibrations are dampened by the coupling and the flexures.

To correctly adjust the position of the roller is necessary to measure the position of it respect to the impression roller and the substrate. Once determined the offset, adjusting the micrometers could place the shaft in the desirable position.

4.3.1.2 Upgrade of the Impression Roller System

As noted in Chapter 3, the precision shaft and the bushing determine the repeatability of the parallelism of the impression roller. Especially, the linear bearing used last year allows a 2 degree self-alignment, which leads to un-repeatable movement of the precision shaft.

The new impression roller system updated or modified following parts or design:

1. Update of the precision shaft (see figure 52). The new shaft adopted in the system have better straightness (0.001"-0.002" per foot), surface hardness (case hardened with minimum hardness depth 0.06") and larger outside diameter (1" compare to 0.75" of previous precision shaft)

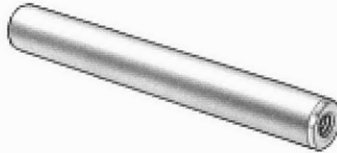


Figure 52: The Updated Precision Shaft

2. Update of the linear bearings (see figure 53). Two closed fixed-alignment ball bearings make them a good solution for vertical linear motion applications with no shaft misalignment. They have end seals to keep lubricants in and dirt out. More importantly, compare to previous linear ball bearing, the updated one has double length to guarantee the repeatable movement of the precision shaft.

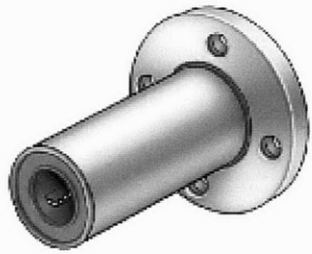


Figure 53: The updated Linear Ball Bearing

3. Update of the assembly. The previous impression roller system has two micrometer-heads to lift up the impression roller (refer to figure 24); such design requires two micrometer-heads to adjust exactly same distance in order to make sure the repeatable movement at both ends of the precision shaft. The updated design of assembly only uses one micrometer-head to move it to the center; therefore, with the confinement of the linear bearings and precision shafts, the impression roller has high repeatability of parallelism.

4.3.2 Print Quality and Comparison with Previous R2R System

The updated design of R2R system significantly improves the repeatability and accuracy of the printing process. Firstly, the updated wrapping process minimized the misalignment and evenly distributed the distortion of the stainless steel sheet while wrapping and hence improved the quality of the features on the stamp. Secondly, 5 degree-of-freedom adjustment design of flexure

enable the highly parallel contact between the impression roller and the print roller, which greatly improve the print quality especially for the materials require sensitive pressure control. Lastly, the updated impression roller system improved the repeatability of the parallelism of the impression roller, which also improves the print quality and is extremely important to multi-layer printing process. In this section, three measurements will be carefully explained: the alignment of the impression roller and the printer roller, repeatability of the parallelism of the impression roller and the distortion of the print feature.

4.3.2.1 Parallelism Between the Impression Roller and the Print Roller

Compared to last year, the updated impression roller system and the flexure designed this year can provide much better parallelism between the impression roller and the print roller. For example, under the pressure of 27 lbs, the printed areas using updated system has a very parallel strip of printed area. As shown in figure 54, with the same length of contact area, the width difference from the top to the bottom using last year's print system is 2.5mm^[4], and the width difference shown in updated system is less than 0.1 mm.

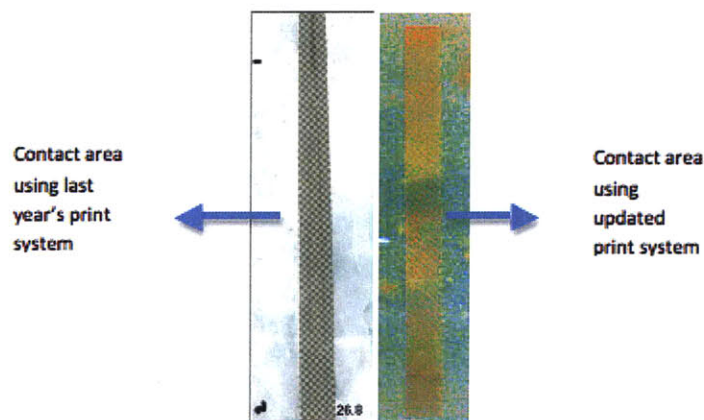


Figure 54: Comparison of Tapered Contact Areas Using Previous and Updated Print System

4.3.2.2 Repeatability of the Parallelism of the Impression Roller

To test the repeatability of updated system, the impression roller is lifted up and then put down and the numbers at both ends of the impression roller are read. The setting is shown in figure 55. Twenty samples are collected for each system.



Figure 55: Setup for The Repeatability of the Parallelism Test

The test result of the previous impression roller system is shown in figure 56. The result showed that the displacement got larger as the experiment went on and the result of samples is not normally distributed. Therefore, it is hard to forecast the average and standard deviation of the displacement. But as the chart shows, the displacement could be at least 0.05mm.

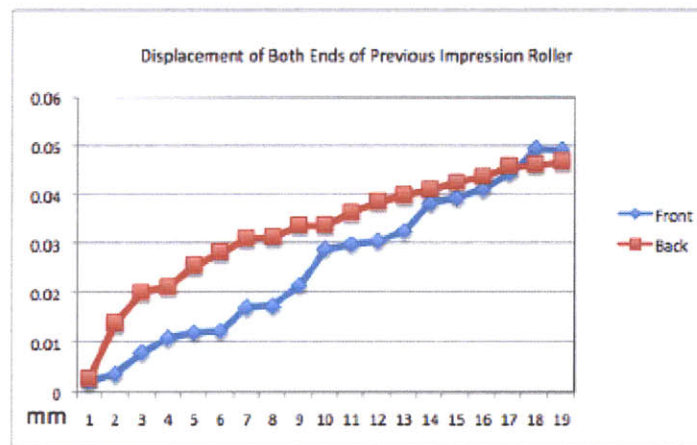


Figure 56: Test Result of the Repeatability of Parallelism for Previous Impression Roller System

The test result of the update impression roller system is shown in figure 57. The result showed that the displacement varied within $5\mu\text{m}$ and the test points are normally distributed based on QQplot test. The statistical result of the measurement is shown in table 2.

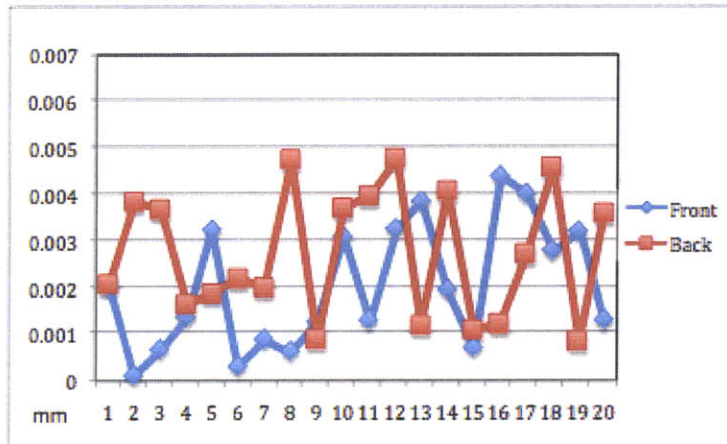


Figure 57: Test Result of the Repeatability of Parallelism for Updated Impression Roller System

Table 2 Repeatability Test of Updated System

Unit: μm	Updated System	
	Front Roller	Back Roller
Average	2.0	2.7
Standard Deviation	1.2	1.3
COV	0.62	0.49
Standard Error	0.26	0.27

In the actual printing process, especially the multi-layer printing process, which require impression roller to move up and down repeatedly, the motion is precisely controlled by the micrometer head. Therefore, the up and down motion is very stable and smooth. After taking the repeatability test using micrometer head to control the motion, the average displacement and the standard deviation at both ends are less than $1\mu\text{m}$.

4.3.2.3 Distortion of Feature in Monolayer Printing

As stated in methodology chapter, the 200mmx200mm printed area on the substrate is divided into 5x5 squares and then measure the dimension of pixels within each square. The result is shown in Table 3, and cell denotes the average length and width of randomly-chose 5 pixels

Table 3 The Dimension of Pixels in a5x5 Matrix

(130.6, 39.78)	(130.6, 39.78)	(130.4, 39.76)	(130.6, 39.78)	(130.6, 39.76)
(130.5, 39.78)	(130.6, 39.74)	(130.6, 39.78)	(130.6, 39.78)	(130.4, 39.74)
(130.6, 39.78)	(130.6, 39.78)	(130.6, 39.76)	(130.5, 39.78)	(130.6, 39.78)
(130.6, 39.76)	(130.4, 39.74)	(130.6, 39.78)	(130.6, 39.78)	(130.3, 39.78)
(130.6, 39.78)	(130.3, 39.76)	(130.6, 39.78)	(130.6, 39.78)	(130.6, 39.76)



Along the Printing Direction

We could hardly observe any pattern of distortion over the printed area. As shown in figure 58, there is no significant trend along or across the printing direction using the distortion rate.

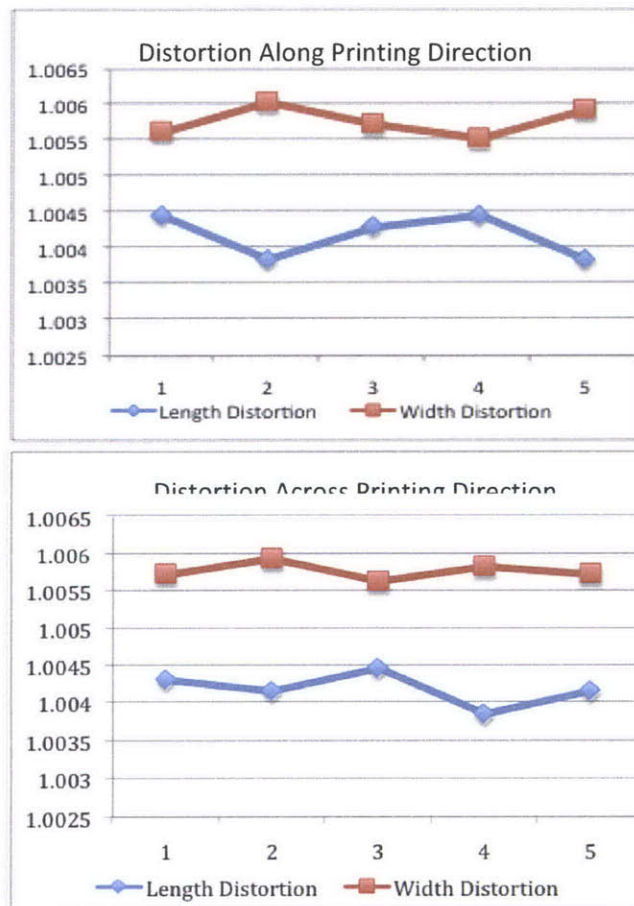


Figure 58: Distortion Along and Across the Printing Direction

However, the distortion of pixels in last year's project had a very special pattern, which was called as diamond pattern ^[4], as shown in figure 59. The reason for such kind of distortion can be attributed to distortion of the backing plate introduced during the manual wrapping process. As mentioned in section 4.2, manually wrapping and locking the stainless steel sheet onto the print roller cannot ensure both ends of the SS sheet were put into the stamp retainer bar in parallel. The unparallel wrapping resulted in stretching the SS sheet along diagonal direction, which directly led to the diamond pattern ^[20]. Thanks to the alignment pins and uniform magnetic force, the wrapping process designed this year can make sure the minimal distortion on the SS sheet and hence minimal distortion of pixels ^[25].

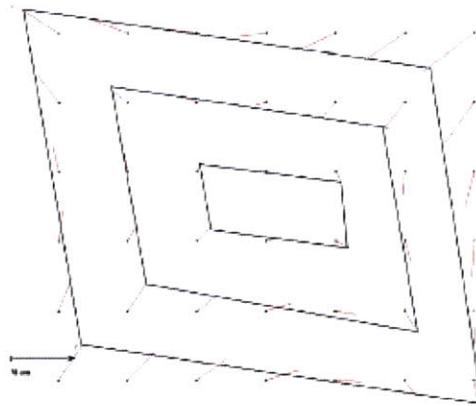


Figure 59: Diamond Pattern of Pixel Distortion in Last Year's Project

4.4 Multi-layer Printing with Updated R2R System

This section is about the multi-layer printing process design and experiment with updated R2R machine. These works are done by Yufei Zhu and me. In his thesis “Design and Manufacturing of High Precision Roll-to-Roll Multi-layer Printing Machine- Machine Upgrade”, multi-layer printing was also mentioned, but in a way of concept design and verification. And the section below focuses on the actual printing process and the result.

4.4.1 Introduction of Multi-Layer Printing Process

The primary target of multi-layer printing is to print the second layer of thiol onto the substrate where a pattern already exists. In order to use the updated R2R machine to realize multi-layer printing, continuous feedback of the registration is a must. The basic process of two-layer printing in this project is to print the first layer using the updated R2R machine without any alignment control. Then wind back the substrate and find the mark on the substrate under the microscope to align the web's position. After that, print the second layer for a certain distance, stop the machine, measure the distance of misalignment between two layers, adjust the print roller correspondingly

and restart printing. As a result, the coming second layer printing should be aligned with the first layer.

The description above is just a general idea of the process; some of the critical processes are developed in following paragraph for better understanding of the precise alignment and feedback control:

1. After the first layer printing, the substrate will not be etched. That means although the substrate has the features that look like the picture shown in figure 60, but those features are not visible. So, marking the general position of each section of pattern is necessary for the etching in the future. The seam between each section of pattern is the area with no stamp on the print roller; in other words, the distance between successive sections is the perimeter of the print roller.

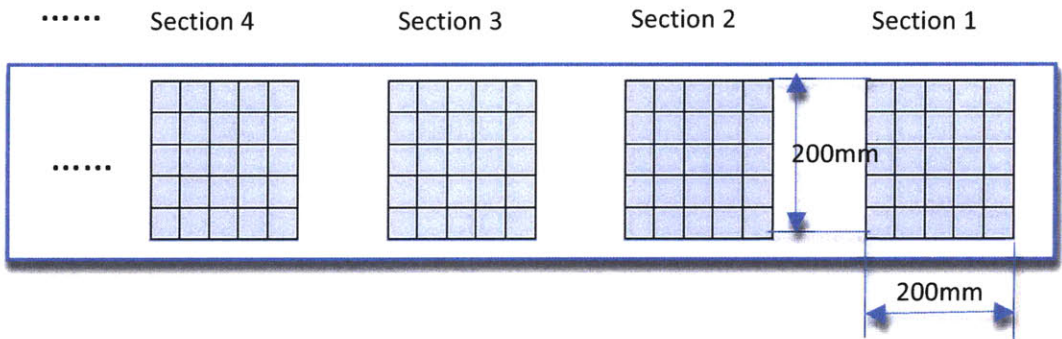


Figure 60: Position of Patterns After First Layer Printing

2. After winding back the printed substrate, the impression roller is lifted up a certain distance using the micrometer head to disengage from the print roller. Then, the substrate is wound forward with tension maintained by the torque of the driving motor in collection module, until the section 1 passes through the print roller (shown in figure 61). The machine is then stopped while keeping the position and tension of the substrate unchanged, and the two microscopes are adjusted to find the marks at the edges of section 1. Currently, Nano Terra does not have the capability to make alignment marks on the stamp, so the pixel on the edge of the substrate is used as the mark to align the position. And those pixels are developed by brushing the etchant onto the substrate.

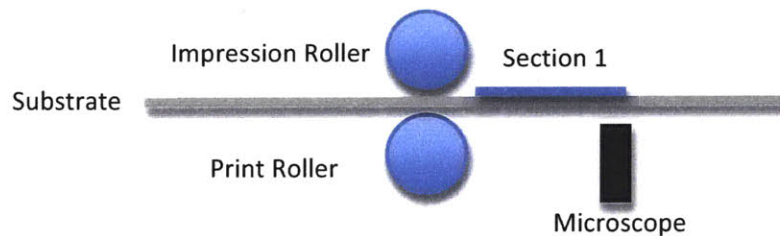


Figure 61: Position Alignment of the First Layer

3. The two microscopes, one at the front of the web and the other at the back, are adjusted to the position where the “mark pixel” is right at the center of the microscope. (See figure 62) Then, the microscopes are locked on the optical table. Since the 200mmx200mm pattern are periodically printed on the substrate, as soon as the microscope find out the “mark feature” at the corners, we know the roller has rotated 360° and the substrate has just float the length of the perimeter of the print roller, which means the relative position of the print roller and the substrate is traceable.

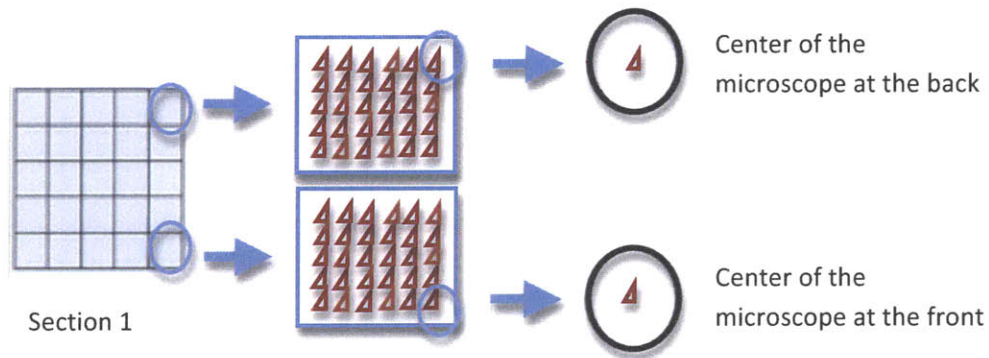


Figure 62: Using Microscope to Align the Position of the Substrate

4. Now, the position of the substrate and the roller is fixed. The impression is moved down to the upper surface of the print roller with the substrate in between. To maintain the calibrated position of the substrate by pressing the impression roller onto its surface the substrate is tightly clamped in feeding part while loosening the substrate in the collection part that compensates the deformation of the substrate caused by impression roller.
5. Then the machine is started to print the second layer on section 2 and then the pixels are developed. The “mark feature” is aligned right at the center of the microscope, so that the relative position of the print roller and the substrate is determined. The displacement of two layers is measured and print roller adjusted to compensate misalignment. For example, in figure 63, the x displacement could be adjusted by rotating the roller in angle of X/R; Y displacement could be adjusted by moving the print roller Y units across the direction of the flying substrate.

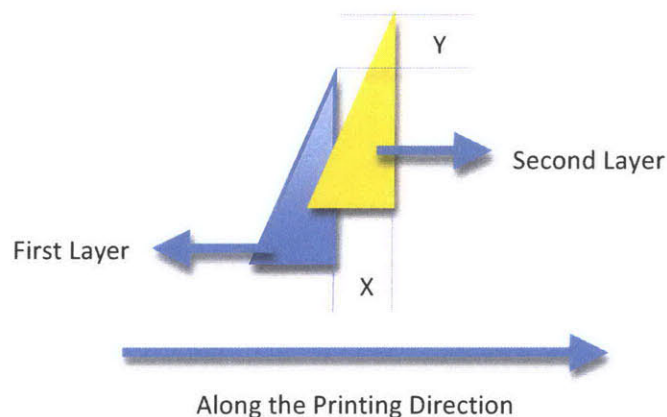


Figure 63: Adjustment of Second Layer printing

6. Ideally, the second layer printing on section 3 should align with the feature on the first layer. If not, re-adjust the print roller and keep printing on section 4. Basically, the machine stops after every printing on each section, align the “mark feature”, monitor the overlap of two layers and make adjustment if needed.

4.4.2 Measurement of Print quality

In general, we performed the multi-layer printing experiment by following the process mentioned in section 4.4.1, however due to some equipment limitations and time constraints, we made some adjustment to simplify the process:

1. Because we could only set up one monitor to link the microscope, we only used one microscope to measure the displacement.
2. It usually takes a very long time to develop the pixels while printing, therefore, instead of using the pixel as the marker, we printed a series of “+“ on both edges of the substrate for alignment.
3. Instead of printing all the features on the first layer, we only printed the first layer with 1 revolution of the print roller and then wound back the substrate to print the second layer.

It is important to note that the multi-layer printing process should follow the descriptions in section 4.4.1, which was the standard process in this project. But because we had to have our first print of multi-layer within very limited time period, we adopted a comparatively rough way to make our first test.

The printed feature is shown in figure 64, which is the central part of the 200mmx200mm print area, and we could easily tell a serious misalignment of two layers.

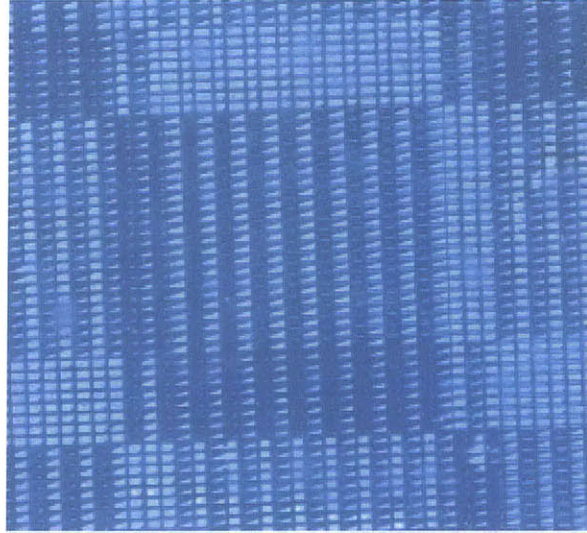


Figure 64: Multi-Layer Printing Result

In order to correctly measure the displacement of two layers, we tried to measure four corners of print area. However we could only get three points out of four, because the printed two layers have the relative position like the picture shown in figure 65. The point at top left is out of the substrate because of the angel between two layers. In the picture, the lower right corner showed $1017\mu\text{m}$ displacement along the printing direction and $113\mu\text{m}$ displacement across the printing direction. The top right corner had the displacement of $1582\mu\text{m}$ along the printing direction and $162\mu\text{m}$ across the printing direction. The lower right corner had displacement of $2962\mu\text{m}$ along the printing direction and $3149\mu\text{m}$ across printing direction.

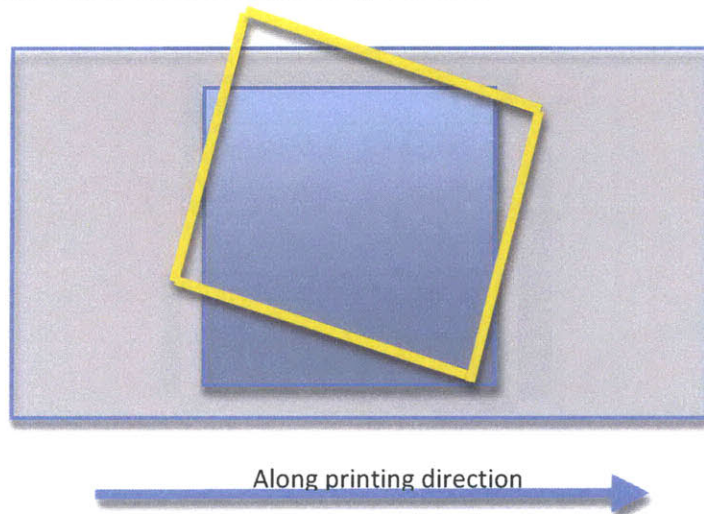


Figure 65: Relative Position of Two Layers

The microscope used to detect the alignment mark was set up at the lower right corner and that is the reason why this corner had the lowest displacement among all three points. When finishing

the first layer printing, the substrate was rewound back to realign its position, however the motion of substrate was not repeatable which means when the substrate was wound back its position changed. Since the initial alignment of the second layer had an angle displace over the first layer, the displacement along the printing direction was amplified by the initial angle and caused a big displacement at the lower left corner.

Although our first result is very good , going through the multi-layer printing process helped us to check whether the process is feasible or not and discover the sources of errors that built up the displacement between two layers. In general, the process worked well: we can adjust the horizontal position of the substrate and the position of the print roller to align two layers with the aid of microscope. Below are the sources of errors that could be modified to significantly improve the alignment of two layers:

1. The main source of the displacement along the printing direction is the step loss of the motor. We used stepper as our driver of the print roller, and this stepper was set up as 2000 steps per revolution. Based on our test of this stepper, we found that on average this stepper lost 4 steps per revolution. Since the print roller had diameter of 125.73mm, those 4 steps loss contribute to $988\mu\text{m}$ displacement along the printing direction at the starting point (lower right corner at figure 66).
2. The microscope we used in this experiment, as shown in figure 6, is a very basic one called Handi-Scope, made by Micro Photonics Inc. Although it has zoom ratio of 40 and 140, the light source is not strong enough to find the mark under 140-zoom ratio. In addition, the quality of the lens is not good enough to observe clear edge of the pixel. Last, the software of this camera does not provide the function of measurement, which means that we were using eyeball to tell whether the mark was in the right position.



Figure 66: Microscope Used for Multi-Layer Printing

3. We were only using one microscope to detect the position of mark, so that it was very difficult to find the angel error across the substrate. If we had time to take another experiment, we would use two microscopes to find marks and adjust the position of the print roller to compensate the substrate's displacement.

4. Last but not the least; the movement of the substrate is not repeatable. Although we could adjust the print roller for initial points' compensation, the waggle of the substrate would cause misalignment during the printing process. And this will be a big problem if continuous multi-layer printing is required.

5 Summary and Future Work

In the project of 2009, we systematically updated the prototype R2R machine to improve its overall accuracy and repeatability. More specifically, the stamp casting device we designed was able to cast the stamp with a flatness of $67\mu\text{m}$ as the range ^[24]; the upgraded stamp wrapping mechanism could attach a backing plate with PDMS onto the print roller with uniform force and good alignment ^[25]; a new flexure design allowed five degree-of-freedom fine adjustment of the stamp roll with very high repeatability ^[26]; the new impression roller system had a repeatability of parallelism in less than $1\mu\text{m}$. In addition, we had our first experiment on multi-layer printing with the updated machine to demonstrate its capability and the multi-layer printing process feasibility.

During the design and experiment process, we found some opportunities to improve the performance of the machine. However, due to time and resource constrains, we could not implement all of those opportunities. Below is the future work that we think could be helpful to upgrade the machine to a next level.

Measurement

- Angular misalignment measurement in multi-layer printing is helpful to study the overall displacement of two layers.

Impression Roller System

- The soft sleeve on the impression roller should be updated to a seamless sleeve, which would improve the print quality by guaranteeing continuous uniform pressure applied on the contact area of the print roller and impression roller.

Multi-layer Printing Process

- A web motion study is essential to web control system and the multi-layer printing. It is important to know whether the web motion has systematic or random error when it is wound back and force, so that the print roller adjustment system could correspondingly adjust its position to produce the best alignment.
- Web control and a feedback system is very critical to multi-layer printing process. In our project, the web was assumed to have no movement across the printing direction. However, that is not the real case. If a mechanical design could confine and control the web movement, the accuracy of multi-layer printing will be significantly improved.

- An easy way to improve the multi-layer printing quality is to use microscopes with high resolution and zoom ratio. Moreover, an optical control and measurement system for the microscope could help to precisely measure the displacement of two layers with high resolution and hence give the right order for motor adjustment.
- A closed- loop feedback control system might be an optimal way to have good quality of multi-layer print. The system could measure the displacement of two layers without stopping the machine and automatically adjust the print roller to align its position for continuous multi-layer printing.

6 Reference

- [1] Xia, Y. and Whitesides, G. M., 1998, "Soft Lithography", *Annual Review Mater. Sci.* 1998. 28:153–84
- [2] Nano Terra Inc, <http://www.nanoterra.com/i/self_assembly_diagram_1.gif>. Accessed 8/1/2008.
- [3] Michel, B. et al., 2000, "Printing Meets Lithography: Soft Approaches to High resolution Patterning", *IBM Journal of Research and Development*, 45(5)
- [4] Stagnaro, A.; "Design and Development of a Roll-to-Roll Machine for Continuous High-Speed Micro-contact Printing"; Massachusetts Institute of Technology, 2008
- [5]. Z.-Q. Gong and K. Komvopoulos. Effect of surface patterning on contact deformation of elastic-plastic layered media. *Journal of Tribology*, 125(1):16-24, 2003.
- [6] K. L. Johnson. *Contact Mechanics*. Cambridge University Press, 1987.
- [7] J. N. Israelachvili. *Intermolecular and surface forces*. Academic Press, 2003.
- [8] K. L. Johnson, K. Kendall, and A. D. Roberts. Surface energy and the contact of elastic solids. *Proceedings of the Royal Society of London Series A, Mathematical and Physical Sciences*, 324(1558):301-313, 1971.
- [9] M. Forster, W. Zhang, A. J. Crosby, and C.M. Stafford. A multilens measurement platform for high-throughput adhesion measurements. *Measurement Science and Technology*, 16(1):81-89, 2005.
- [10] M. K. Chaudhury and G. M. Whitesides. Direct measurement of interfacial interactions between semispherical lenses and flat sheets of poly(dimethylsiloxane) and their chemical derivatives. *Langmuir* 7(5):1013-1025, 1991.
- [11] A. A. Griffith. The phenomena of rupture and flow in solids. *Philosophical Transactions of the Royal Society of London. Series A, Containing Paper of a Mathematical or Physical Character*, 221:163-198, 1921.
- [12] D. Maugis and M Barquins. Fracture mechanics and the adherence of viscoelastic bodies. *Journal of Physics D: Applied Physics*, 11(14):1989-2023, 1978.
- [13] Brian Cotterell, Gordon Williams, John Hutchinson, and Michael Thouless. Announcements of a round robin on the analysis of the peel test. *International Journal of Fracture*, 114(3):9-13, 2002.

- [14] Laser Triangulation Sensors, <[Http:// www.sensorland.com](http://www.sensorland.com)>, Accessed on 08/1/2009
- [15] Interferometry, <[Http://www.wikipedia.com](http://www.wikipedia.com)> accessed on 08/1/2009
- [16] Alexander H. Slocum, Precision Machine Design, Michigan: Society of Manufacturing Engineers Dearborn, 1992
- [17] MTI instrument Inc. <[Http://www.mtiinstruments.com/](http://www.mtiinstruments.com/)>, Optical Fiber, accessed on 08/2009
- [18] Giallorenzi et al., Optical Fiber Sensor Technology, IEEE J. Auantum Electron., Vol. QE-18, No.4 1982,pp.
- [19] Pawley JB (editor) (2006). Handbook of Biological Confocal Microscopy (3rd ed.). Berlin: Springer.
- [20] Khanna,K; “Analysis of the Capabilities of Continuous High-Speed Microcontact Printing”; Massachusetts Institute of Technology, 2008
- [21] Shen, Shawn. “Design and Analysis of High-speed Continuous Micro-Contact Printing”. Massachusetts Institute of Technology. August 19, 2008.
- [22] Sriram Krishnan, “On the Manufacture of Very Thin Elastomeric Films by Spin-Coating”, Massachusetts Institute of Technology. September 2007
- [23] Con-Focal Microscopy, <[Http://www.wikipedia.com](http://www.wikipedia.com)>, accessed on 08/1/2009
- [24] Zhu, Yufei. “Design and Manufacturing of High Precision Roll-to-Roll Multi-layer Printing Machine- Machine Upgrade”. Massachusetts Institute of Technology. August 18, 2009.
- [25] Charudatta Datar, “Design and Development of High Precision Elastomeric-Stamp Wrapping System for Roll-to-Roll Multi-Layer Microcontact Printing”, Massachusetts Institute of Technology. August 18, 2009.
- [26] Paolo Baldesi, “Design and Manufacturing of High Precision Five Axis Positioning system for Roll-to-Roll Micron Contact Printing”. Massachusetts Institute of Technology. August 18, 2009.